



# Dynamics of a pipeline buried in loosely deposited seabed to nonlinear wave & current

Jianhong Ye<sup>a,\*</sup>, Kunpeng He<sup>a,b</sup>

<sup>a</sup> State Key Laboratory of Geomechanics and Geotechnical Engineering, Institute of Rock and Soil Mechanics, Chinese Academy of Sciences, Wuhan, 430071, China

<sup>b</sup> University of Chinese Academy of Sciences, Beijing, 100049, China

## ARTICLE INFO

### Keywords:

Fluid-structure-seabed interaction (FSSI)  
Pore pressure build up  
Residual liquefaction  
Loosely deposited seabed soil  
Sinking and floating of pipeline  
Seabed liquefaction  
Wave & current  
Pastor-Zienkiewicz Mark III  
FSSI-CAS 2D

## ABSTRACT

Submarine pipeline is a type of important infrastructure in petroleum industry, used for transporting crude oil or natural gas. Understanding of the dynamics characteristics under hydrodynamic loading is crucial for engineers when assessing the stability of offshore pipelines in their designed service period. In this study, taking the integrated numerical model FSSI-CAS 2D as the tool, the nonlinear ocean wave & current-induced dynamics of a shallowly buried submarine steel pipeline and its surrounding loosely deposited seabed soil is numerically investigated. The excellent soil model Pastor-Zienkiewicz-Mark III (PZIII) is adopted to describe the complicated mechanical behaviour of loose seabed soil under cyclic loading. Computational results indicate that the shallowly buried submarine pipeline eventually significantly float up, and extrude the seabed soil over the pipeline driven by the gradually increased buoyancy on the pipeline caused by the accumulation of pore pressure around the pipeline, making the seabed over the pipeline hunch significantly. As a result, considerable deformation occurs in the seabed soil surrounding the pipeline. Two effective stress-based criterion are proposed to judge the occurrence of soil liquefaction. Adopting the two criterion, it is found that the surrounding seabed soil around the pipeline does not become liquefied; only stiffness softening has occurred in it. However, the soil in the upper seabed with shallow depth away from the pipeline becomes liquefied with a liquefaction depth 1.2–1.5 m. Comparative analysis indicates that the pipeline transporting natural gas floats upward with a much greater displacement than that if crude oil is transported. The computational results show that the integrated model FSSI-CAS 2D has successfully and subtly captured a series of nonlinear physical phenomena of the intensive interaction between pipeline and its surrounding seabed soil. Finally, it is indicated that the integrated model FSSI-CAS 2D has an advantage to investigate the complicated interaction between fluid-structure-seabed foundation.

## 1. Introduction

Submarine pipeline is an important type of infrastructure in petroleum industry. It is broadly used for transporting crude oil or natural gas. Nowadays, several hundreds of thousands kilometers of submarine pipelines would have been built worldwide. The stability of submarine pipelines is absolutely the precondition for ensuring their normal service performance in the designed service period. However, submarine pipelines are vulnerable under the attacking of extreme ocean wave or strong seismic wave due to the breaking or lateral buckling caused by the liquefaction of seabed foundation. Some such kind of catastrophic failures have been reported in the past decades, e.g. Christian et al. (1974) reported that an underwater pipeline for a nuclear plant with a diameter 3.05 m and a buried depth about 3 m in Lake Ontario has failed for

several times, apparently due to soil liquefaction; Herbich et al. (1984) also reported that a pipeline with a diameter 3.05 m was found to float up to the bed surface after an extreme storm in the construction period. Therefore, it is necessary and meaningful to understand the responding dynamics characteristics of submarine pipelines under cyclic loading applied by ocean waves or seismic waves.

Generally, the instability of submarine pipelines could be attributed to scouring, ocean wave action or seismic wave attacking. On the seismic dynamics of submarine pipeline shallowly buried in seabed foundation, scientists and engineers actually have paid little attention on it. Only a few works have been previously conducted. A latest brief literature view on the seismic dynamics of submarine pipelines is available in Zhang et al. (2019). On the scouring of seabed floor near to submarine pipelines, some valuable works also have been conducted to understand the

\* Corresponding author.

E-mail addresses: [yejianhongcas@gmail.com](mailto:yejianhongcas@gmail.com), [Jhye@whrsm.ac.cn](mailto:Jhye@whrsm.ac.cn) (J. Ye).

<https://doi.org/10.1016/j.oceaneng.2021.109127>

Received 19 March 2020; Received in revised form 18 February 2021; Accepted 4 May 2021

Available online 18 May 2021

0029-8018/© 2021 Elsevier Ltd. All rights reserved.

mechanism under the action of ocean wave and current (Larsen et al., 2016; Kiziloz et al., 2013; Bayraktar et al., 2016; Fredsoe, 2016). However scouring is not the focus of this study.

On the ocean wave-induced dynamics of submarine pipeline, a series of research works also have been previously conducted, and a great number of literature are currently available. The research method mainly includes analytical solution, numerical modelling and laboratory wave flume test. On the aspect of analytical solution, numerical modelling of the dynamics of pipeline, A latest brief literature view is also available in Zhang et al. (2019). However, most of previous works were limited to the condition that the seabed soil was deemed as poro-elastic medium (MacPherson, 1978; Magda, 1992; Duan et al., 2017). In fact, there is another types of seabed soil widely existed in offshore area in the world. It is loosely deposited seabed soil, in which pore pressure could build up significantly under hydrodynamic loading (Summer et al., 2006b), resulting in seabed soil becoming liquefied. Recently, the wave-induced dynamics of pipeline buried in loose seabed soil is tentatively investigated (Zhao et al., 2018) adopting some empirical-based soil models, such as the soil model proposed by Seed (Seed and Rahman, 1978; Martin and Seed, 1984). There were also a few investigations adopting advanced soil model, such as PZIII model proposed by Zienkiewicz et al. (1999) to do such work (Dunn et al., 2006; Zhang et al., 2011). Unfortunately, the intensive interaction between pipeline and seabed foundation, the large deformation occurred in loosely deposited surrounding soil, and the sinking/floatation of pipeline have not comprehensively demonstrated in these works.

On the aspect of the laboratory wave flume test, there are also several typical works are available for the dynamics of pipeline buried in loose sandy bed. Summer B M have conducted a series of wave flume tests to investigate the dynamics of a pipeline and its surrounding sandy soil (Sumer et al., 1999; Summer et al., 2006b, a). They conformed that the surrounding sandy soil of pipeline can become liquefied, and the pipeline can sink or float up under hydrodynamic loading. Teh et al. (2003) also performed a great number of wave flume tests to observe the process of pore pressure accumulation, the liquefaction of sandy bed, as well as the sinking of pipeline. Based these tests, Teh et al. (2006) proposed a formulation to predict the sinking depth of offshore pipeline. Zhou et al. (2011) also conducted a number of large scale wave flume tests for the problem of wave-pipeline-seabed soil interaction. However, only the wave-induced excess pore pressure was measured and analyzed in their work. Observation on the soil deformation and on the sinking or floatation of pipeline was not performed at all. Neelamani and Al-Banaa (2012) performed a series of wave flume tests to observe the variation of random wave-induced force on pipeline buried in different types of soil. It was found that the permeability of soil and the buried depth had significant effect on the wave-induced force on underwater pipelines. Most recently, Miyamoto et al. (2020) perform a number of important wave flume tests in a drum centrifuge for the pipeline-soil interaction problem, which owns breakthrough and milestone meaning in the authors' opinion. In their tests, ocean waves are generated by a vibrating paddle. Then the generated waves propagate along a ring channel in the drum centrifuge, and apply hydrodynamic loading to the loose sandy bed in which a pipeline is shallowly buried. Wave-induced soil liquefaction and the floatation of pipeline are also clearly observed in these tests. Miyamoto et al. (2020)'s work will be a typical work in the literature of offshore geotechnics. All these laboratory wave flume tests previously conducted are beneficial for the engineers and scientists to understand the characteristics and mechanism of the pipeline-loose seabed foundation interaction under hydrodynamic loading.

It is indicated by a number of previous failure cases, such as that reported by Christian et al. (1974) and Herbich et al. (1984), that the upheaval bulking of buried pipelines is one of the most important instability mechanism in engineering practice. In order to avoid the floatation of buried pipelines, increasing the buried depth and the specific gravity (SG) of submarine pipelines are the two common measures used in the design of engineering. Current guideline on the SG of

submarine pipelines is generally suggested to be limited into 1.7 to 1.8. However, the origins of such recommendation are not clear, as claimed by Bizzotto et al. (2017b). Powell et al. (2002) proposed a value range of 1.5–1.7 for the SG of submarine pipelines based on a series of physical model tests. If the potential of floatation is highly possible, extra engineering measures, such as rock dumping could be adopted to avoid the possible upheaval bulking, as pointed out by Cathie et al. (2005) and Cowie and Finch (2001). It has been recognized that the upheaval bulking of submarine pipeline can be caused by (1) The thermal expansion of the steel wall of pipeline when transporting elevated temperature substances during operating period; (2) The operational defects in the process of pipeline laying, ploughing or jetting, and backfilling; (3) The significant accumulation of pore pressure and the resultant soil softening or liquefaction in the surrounding seabed soil induced by the environmental dynamic loading, such as ocean wave and seismic wave. As a result, the buoyancy applied on pipelines becomes much greater, and the upheaval resistance of the surrounding soil reduces significantly, which could directly lead to submarine pipelines are prone to uplift. For the first and second mechanism stated above where there is no dynamic environmental loading involved, there have been a series of numerical or laboratory investigations to study the uplift failure mechanism of submarine pipelines (Bizzotto et al., 2017a, 2017b; Cowie and Finch, 2001; Cathie et al., 2005; Roy et al., 2018; Cheuk et al., 2008; Bransby et al., 2001; Berghe et al., 2005; Newson and Deljoui, 2006). However, there are only few works have been conducted for the floatation of pipelines under the dynamic loading of ocean wave or seismic wave (Miyamoto et al., 2020), so far as we know. In this study, we will focus on the above mentioned third mechanism involving the ocean wave or seismic wave.

It is known that ocean wave is a kind of significant and non-ignorable environment loading for marine structures, such as submarine pipelines. It brings great threat to the stability of offshore structures constructed on or shallowly buried in loosely deposited seabed foundation. In this study, taking the integrated numerical model FSSI-CAS 2D as the tool, the wave & current-induced dynamics of a submarine steel pipeline shallowly buried in loose seabed foundation is comprehensively investigated. The analysis results could further improve the understanding of ocean engineers and scientists on the dynamics of submarine pipeline buried in loose seabed foundation under hydrodynamic loading.

## 2. Numerical model and constitutive model

Dynamic Biot's equation known as “ $u - p$ ” approximation proposed by Zienkiewicz et al. (1980) are used to govern the dynamic response of porous seabed soil under cyclic loading:

$$\frac{\partial \sigma'_x}{\partial x} + \frac{\partial \tau_{xz}}{\partial z} = -\frac{\partial p}{\partial x} + \rho \frac{\partial^2 u_s}{\partial t^2}, \quad (1)$$

$$\frac{\partial \tau_{xz}}{\partial x} + \frac{\partial \sigma'_z}{\partial z} + \rho g = -\frac{\partial p}{\partial z} + \rho \frac{\partial^2 w_s}{\partial t^2}, \quad (2)$$

$$k \nabla^2 p_s - \gamma_w n \beta \frac{\partial p}{\partial t} + k \rho_f \frac{\partial^2 \varepsilon_v}{\partial t^2} = \gamma_w \frac{\partial \varepsilon_v}{\partial t}, \quad (3)$$

where  $(u_s, w_s)$  are the soil displacements in horizontal and vertical direction, respectively;  $n$  is soil porosity;  $\sigma'_x$  and  $\sigma'_z$  is the effective normal stresses in the horizontal and vertical direction, respectively;  $\tau_{xz}$  is the shear stress;  $p$  is the pore water pressure;  $\rho = \rho_f n + \rho_s (1 - n)$  is the average density of porous seabed;  $\rho_f$  is the fluid density;  $\rho_s$  is solid density;  $k$  is the Darcy's permeability;  $g$  is the gravitational acceleration,  $\gamma_w$  is unit weight of water and  $\varepsilon_v$  is the volumetric strain. In Equation (3), the compressibility of pore fluid ( $\beta$ ) and the volumetric strain ( $\varepsilon_v$ ) are defined as

$$\beta = \left( \frac{1}{K_f} + \frac{1 - S_r}{p_{w0}} \right), \quad \text{and } \varepsilon_v = \frac{\partial u_s}{\partial x} + \frac{\partial w_s}{\partial z}, \quad (4)$$

where  $S_r$  is the degree of saturation of seabed,  $p_{w0}$  is the absolute static pressure and  $K_f$  is the bulk modulus of pore water, generally,  $K_f = 2.24 \times 10^9 \text{Pa}$ . Here, the compressibility of pore fluid  $\beta$  is taken to consider the unsaturation of seabed soil, which is only applicable for the nearly saturated soil.

FE method is utilized to solve the above governing equations (1)–(3), and Generalized Newmark Scheme (implicit scheme) is adopted to calculate the time integration when solving the above governing equations (Chan, 1988). For the problem of Fluid-Structure-Seabed Interaction (FSSI), an integrated/coupled numerical model FSSI-CAS 2D was developed by the authors (Ye, 2012). In FSSI-CAS 2D, the wave motion and the porous flow in porous seabed is governed by VARANS equation (Hsu et al., 2002). Meanwhile, the dynamic behaviour of offshore structure and its seabed foundation is governed by the above Equations (1)–(3). A coupled algorithm was developed to couple the VARANS equation and Biot’s dynamics equation together. More detailed information about FSSI-CAS 2D can be found in Ye et al. (2013b), and Ye (2012).

Void ratio  $e$  and related Darcy’s permeability  $k$  of soil generally is variational depending on the deformation of soil. In computation, the wave-current induced variation of void ratio of seabed soil is considered, following

$$e_{n+1} = (1 + e_n) \exp\left(\frac{\Delta p}{Q} + \Delta \varepsilon_{vs}\right) - 1 \quad (5)$$

where  $n$  stands for  $n^{\text{th}}$  time step,  $\Delta p$  is the incremental pore pressure,  $\Delta \varepsilon_{vs}$  is the incremental volumetric strain of soil, and  $Q = 1/\beta$  is the compressibility of pore water. The above equation is established from the perspective of large deformation. Correspondingly, the permeability of seabed soil  $k$  variates following

$$k = C_f \frac{e^3}{1 + e} \quad (6)$$

where  $C_f = k_0 \frac{1+e_0}{e_0^3}$  is an empirical coefficient (Miyamoto et al., 2004), in which  $e_0$  and  $k_0$  is the initial void ratio and permeability.

In this study, an excellent soil model Pastor-Zienkiewicz-Mark III (PZIII) proposed by Pastor et al. (1990) is adopted to describe the dynamic behaviour of loose seabed soil surrounding pipeline. The reliability of PZIII has been validated by a series of laboratory tests in which monotonic and cyclic loading are both involved, especially the centrifuge tests in the VELACS project (Zienkiewicz et al., 1999). This model is one of the heritages of Olek Zienkiewicz (Pastor et al., 2011).

### 3. Verification for pipeline-seabed interaction

The developed integrated model FSSI-CAS 2D has been widely validated in previous literature published by the authors (Ye et al., 2013b), involving analytical solutions, a series of wave flume tests, and one centrifuge test. It also has been successfully applied to study the dynamics of large-scale breakwater and its seabed foundation, involving breaking waves (Ye et al., 2014), tsunami waves (Ye et al., 2013a), as well as seismic wave (Ye and Wang, 2015). It is proved that the integrated numerical model FSSI-CAS 2D is applicable for the analysis of the dynamics of offshore structures and their seabed foundation. However, pipeline was not involved in previous verification cases. Here, the reliability of FSSI-CAS 2D for the problem of pipeline-seabed interaction is further illustrated adopting some previous wave flume test results.

#### 3.1. Elastic seabed

Turcotte (1984) conducted a series of wave flume tests for the

problem of pipeline-seabed interaction at Cornell University. These test results have been widely adopted to examine the reliability of some analytical solutions (Zhou et al., 2013) and numerical models (Luan et al., 2008; Zhang et al., 2011). In this section, Turcotte (1984)’s test results are also adopted to verify the reliability of FSSI-CAS 2D for the problem of pipeline-seabed interaction.

In Turcotte (1984)’s test, an empty steel pipeline with a SG (specific gravity) of 0.907 was buried in a sandy bed installed in a wave flume. A series of water waves were generated to apply cyclic loading on the surface of the sandy bed. Totally eight water pressure sensors were uniformly installed around the pipeline to record the wave-induced pressure. The dimension and the property parameters of the sandy bed, as well as the pipeline given by Turcotte (1984) are listed in Table 1. The water depth in the wave flume was 0.533 m. Three kinds of water wave with different wave heights and wave periods were generated in tests. The integrated model FSSI-CAS 2D is used to reproduce the experimental process of these wave flume tests adopting poro-elastic soil model. Finally, the reliability fo FSSI-CAS 2D is validated by comparing the numerical results with the test data given by Turcotte (1984).

The comparison between the wave flume test data and the present numerical results for the three kinds of water waves are illustrated in Fig. 1. It can be seen that the numerical results reproduced by FSSI-CAS 2D agree very well with the test results in the cases where the wave height is 14.3 cm or 3.02 cm. In order to further enhance the reliability of this verification, the theoretic results proposed by Cheng (1986) is also given in Fig. 1. It is further found that the numerical results reproduced by FSSI-CAS 2D in the case where the wave height = 5.24 cm, wave period = 0.9 s is greater than the test results. However, the agreement between the present numerical results and the theoretic results proposed by Cheng (1986) is quite well. Overall, it is indicated that the integrated model FSSI-CAS 2D is reliable for the problem of wave-elastic seabed-pipeline interaction.

#### 3.2. Loose seabed

Except for dense elastic seabed, the verification for loosely deposited seabed soil is also necessary for FSSI-CAS 2D. Actually, this verification work has been performed by us (Ye et al., 2013b) in a previous publication. In Ye et al. (2013b)’s work, there were two typical laboratory tests performed by Teh et al. (2003) and Sassa and Sekiguchi (1999) were used to take the verification work. The verification work shown that the integrated model FSSI-CAS 2D is also reliable for the problem of wave-loose seabed-pipeline interaction, so long as an appropriate advanced soil constitutive model is selected, and the model parameters for loose seabed soil is reliably calibrated based on credible laboratory testing data. Based on these verification work in Ye et al. (2013b), the integrated model FSSI-CAS 2D has been successfully applied to

**Table 1**  
Parameters in the wave flume tests conducted by Turcotte (1984).

Parameters	Value	Unit
Sandy bed properties		
Length	4.57	m
Depth	0.826	m
Density of particles	2700	kg/m <sup>3</sup>
Porosity	0.42	–
Permeability	1.1 × 1.0 <sup>-3</sup>	m/s
Young’s modulus	0.64	MPa
Poisson’s ratio	0.33	–
Pipeline properties		
Diameter	0.168	m
Buried depth	0.167	m
Wall thickness	0.01	m
Steel density	7850	kg/m <sup>3</sup>
Young’s modulus	200	GPa
Poisson’s ratio	0.35	–
Specific gravity (SG)	0.907	–

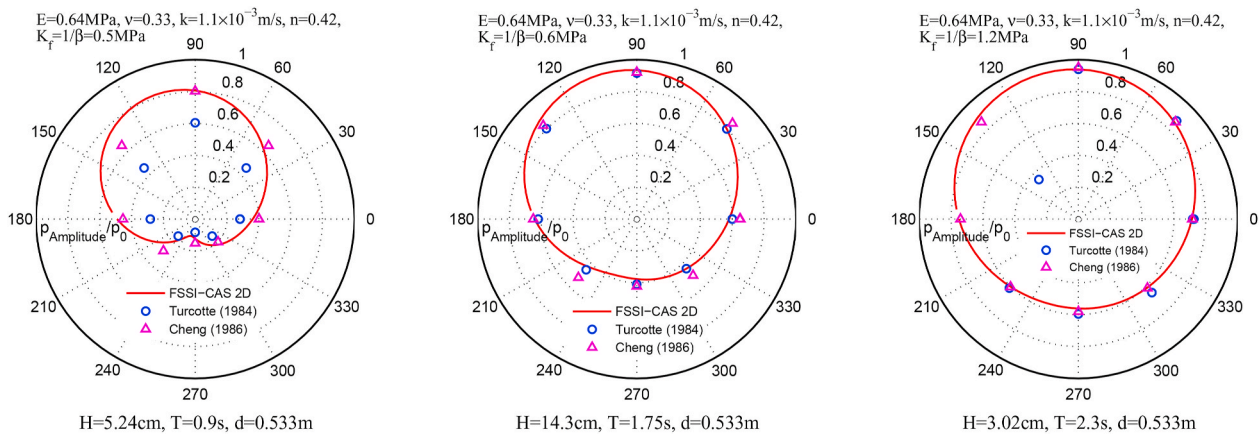


Fig. 1. Comparison between the wave flume test results given by Turcotte (1984) and the present numerical results for the wave-induced dynamic pore pressure around the pipeline ( $E$ : elastic modulus,  $\nu$ : Poisson's ratio,  $k$ : permeability,  $n$ : porosity,  $K_f = \frac{1}{\beta}$ : bulk modulus of pore water,  $H$ : wave height,  $T$ : wave period,  $d$ : water depth).

investigate the dynamics and residual liquefaction of loosely deposited seabed under wave loading (Yang and Ye, 2017, 2018) or seismic wave loading (Ye and Wang, 2016). It is shown that the integrated model FSSI-CAS 2D can describe the progressive liquefaction process and post-liquefaction behaviour of loose seabed soil when an appropriate advanced soil constitutive model is incorporated.

#### 4. Computational domain, boundary conditions and hydrodynamic loading

As demonstrated in Fig. 2, a steel pipeline with a wall thickness of 3 cm with a outer diameter of 800 mm transporting crude oil is buried in the loosely deposited seabed (specific gravity at empty (SG) = 1.113). The water depth  $d$  over the seabed surface is 10 m. The buried depth of the pipeline is 1.0 m (the distance from the pipeline center to the surface of seabed). The computational domain of the seabed foundation is 200 m in length and 20 m in thickness. The pipeline is installed on the symmetrical line  $x = 100$  m.

The bottom of the seabed foundation is fixed both in  $x$  and  $z$  direction. The two lateral sides of the computational domain are also fixed in  $x$  direction, and set free in  $z$  direction. On the surface of the seabed

foundation, the hydrostatic and hydrodynamic water wave pressure is applied. At the meantime, the effective stresses keep zero at all times on the surface of seabed floor, because the seabed foundation is porous. In order to simulate the working status of the pipeline, a pressure with a value of 200 kPa driving the crude oil flowing in the pipeline is applied. Due to the fact that the seabed floor is flat in the computation domain, the hydrodynamic water pressure can be determined by analytical solution. The analytical formulation first explicitly proposed by Ye and Jeng (2012) for the third-order wave-current is used in this study. As a result, the hydrostatic and hydrodynamic water wave pressure applied on the surface of seabed floor is:

$$P(x, t) = \rho_f g d + \frac{\rho_f g H}{2 \cosh \lambda d} \left[ 1 - \frac{\omega_2 \lambda^2 H^2}{2(U_0 \lambda - \omega_0)} \right] \cos(\lambda x - \omega t) + \frac{3 \rho_f H^2}{8} \left\{ \frac{\omega_0 (\omega_0 - U_0 \lambda)}{2 \sinh^4(\lambda d)} - \frac{g \lambda}{3 \sinh 2 \lambda d} \right\} \cos 2(\lambda x - \omega t) + \frac{3 \rho_f \lambda H^3 \omega_0 (\omega_0 - U_0 \lambda)}{512} \frac{(9 - 4 \sinh^2(\lambda d))}{\sinh^7 \lambda d} \cos 3(\lambda x - \omega t) \quad (7)$$

where  $H$  is wave height,  $T$  is wave period,  $d$  is water depth.  $\rho_f$  is the density of sea water,  $g$  is gravity,  $\lambda = L/2\pi$  is wave number, where  $L$  is

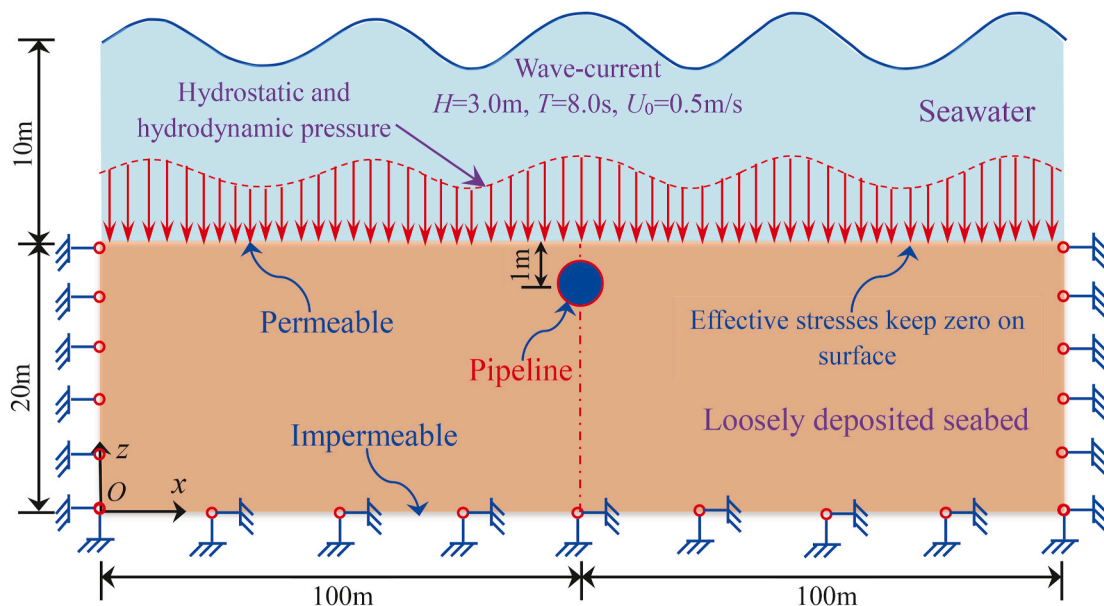


Fig. 2. Schematic diagram of the pipeline-seabed-wave (current) system used in computation.

wave length,  $\omega = T/2\pi$  is angle frequency.  $U_0$  is current velocity. When there is no current in wave ( $U_0 = 0$  m/s), the above third-order solution can be degraded into the classic form of the solution of third-order nonlinear wave. One of the advantages of Equation (7) is that the high nonlinearity of ocean wave in shallow water can be effectively considered. It is noted that the wave-induced seabed scouring, as well as the effect of axial force along the pipeline and the hogging curvature generated in the process of pipeline installation on the dynamics of pipeline and its surrounding seabed soil are all not considered in modelling.

The generated mesh for the pipeline and seabed used in computation is shown in Fig. 3. There are totally 23316 4-nodes elements. In the mesh, the pipeline is treated as impermeable and rigid steel circle (wall thickness = 3 cm), and the transported crude oil is also meshed. Four typical point A, B, C and D around the pipeline labelled in Fig. 3 are chosen as the representatives to analyze the characteristics of dynamics of seabed soil surrounding the pipeline thereafter.

The parameters of the loosely deposited seabed soil for PZIII model are listed in Table 2. They were previously determined by Zienkiewicz et al. (1999) for Nevada sand ( $D_r=60\%$ ,  $D_{50} = 0.14-0.17$  mm,  $C_u = 1.67$  and  $G_s = 2.64-2.67$  coming from Kammerer et al. (2000)) when taking part in the VELACS project. The initial void ratio  $e$ , and saturation of seabed soil used in computation is 0.7372, and 98%, respectively; and they are both uniformly distributed in the computational domain. Correspondingly, the initial permeability is set as  $7.2 \times 10^{-5}$  m/s. Wave height, wave period and current velocity is set as 3.0 m, 8.0s,  $U_0 = 0.5$  m/s, respectively.

## 5. Results

### 5.1. Initial state

Before applying the wave-current loading, there is an initial state for the pipeline-seabed foundation system. This initial state should be taken as the initial condition for the subsequent dynamics analysis. The detailed analysis on the initial displacement, pore pressure and effective stresses of the seabed-pipeline system is available in Zhang et al. (2019), which is just recently published by the authors. Overall, the existence of the pipeline has significant effect on the initial distribution of displacement, and effective stresses in the surrounding seabed soil of the pipeline.

### 5.2. Dynamic displacement of pipeline

Due to the fact that the ocean wave-induced dynamics of loosely deposited seabed soil has been comprehensively investigated adopting advanced elasto-plastic soil model in several previous literature, such as Yang and Ye (2018), Yang and Ye (2017), and Liao et al. (2015), the dynamics of seabed soil far away from the pipeline is not presented any

**Table 2**

Model parameters of loose seabed soil for PZIII in analysis.

Item	Nevada dense sand	Unit
$K_{ev0}$	2,000	[kPa]
$G_{eso}$	2,600	[kPa]
$p'_0$	4	[kPa]
$M_g$	1.32	-
$M_f$	1.3	-
$\alpha_f$	0.45	-
$\alpha_g$	0.45	-
$\beta_0$	4.2	-
$\beta_1$	0.2	-
$H_0$	750	-
$H_{U0}$	40,000	[kPa]
$\gamma_u$	2.0	-
$\gamma_{DM}$	4.0	-

more here. Only the dynamics of the pipeline and its surrounding seabed soil, as well as their interaction are the focus in this study.

The dynamic displacement of the pipeline responding to the wave and current loading is demonstrated in Fig. 4. It is found that the pipeline continuously moves toward to the right side in horizontal direction, accompanied by a regular vibration. And the amplitude of the horizontal vibration increases gradually. At the end of the computation ( $t = 156$  s), the residual horizontal displacement of the pipeline is about 90 mm. The amplitude of the horizontal vibration is about 30 mm. It means that the horizontal vibration of the pipeline is relatively strong under the cyclic loading applied by the wave and current. It is also can be seen that the vertical displacement of the pipeline contains two components as well: residual and oscillatory, respectively. Oscillatory displacement definitely is due to the periodic applying of ocean wave, meanwhile the residual displacement is due to the deformation of surrounding seabed soil. From the perspective of residual vertical displacement. It is observed that the pipeline is sinking before  $t = 80$  s. After that the pipeline continuously floats up. This transition of displacement mode of the pipeline is closely related to the development of residual pore pressure in the loosely deposited surrounding soil of the pipeline under hydrodynamic loading. This vibration and the floatation of pipeline actually have previously been clearly observed in some wave flume tests conducted by Sumer et al. (1999), Teh et al. (2003) and Miyamoto et al. (2020). It is indicated that the integrated model FSSI-CAS 2D can effectively capture the complicated behaviour of shallowly buried pipeline under hydrodynamic loading.

Previous studies (Yang and Ye, 2018; Summer et al., 2006b) have proved from the perspectives of experiment and numerical modelling that the pore pressure in loose seabed soil will build up under cyclic wave loading. In this study, it is also observed that the pore pressure has

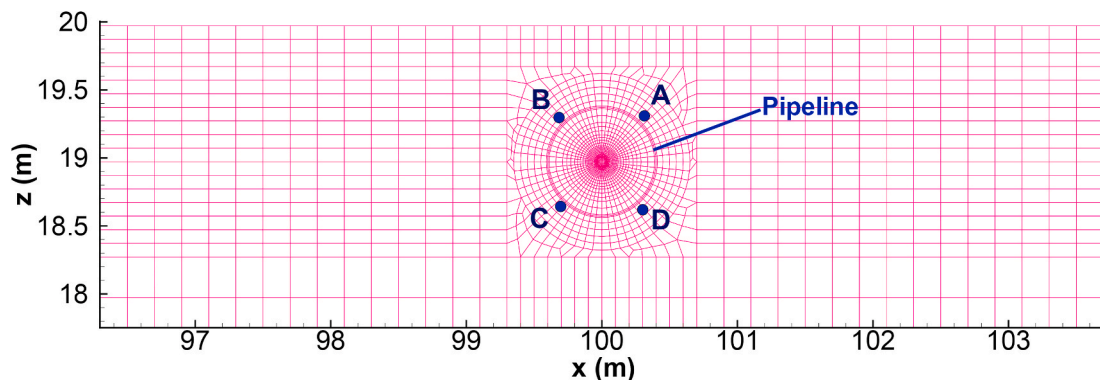


**Fig. 3.** Generated mesh for the pipeline and seabed foundation in computation (Noted: the crude oil transported in the pipeline is also meshed, and only the mesh near to the pipeline is shown).

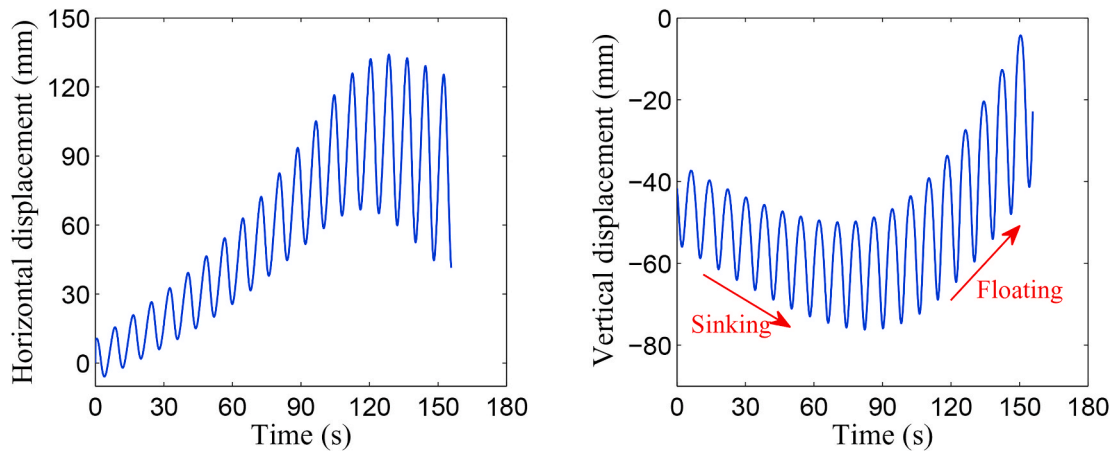


Fig. 4. Time history of the displacement of the steel pipeline responding to the wave & current loading (Noted: there is an initial value in the vertical displacement due to the initial subsiding of the pipeline at the initial state).

built up in the surrounding loose seabed soil under the action of wave and current. As a result, the upward floating force on the pipeline applied by the pore water will gradually become greater and greater in the process of pore pressure accumulation, as illustrated in Fig. 5. In Fig. 5, it can be seen that there is a positive residual value for the horizontal component of the floating force  $F_x$  from the time  $t = 50$  s. This is the reason why there is a residual horizontal displacement towards to the right side. Furthermore, the development of the vertical component of the floating force  $F_z$  is very interesting.  $F_z$  is less than the gravity of the pipeline-oil system in the early stage. At a critical point,  $F_z$  becomes greater than the gravity of the pipeline-oil system, resulting from the wave and current-induced pore pressure build-up in the surrounding loose seabed soil. Just because of this considerable upward floating force applied by the pore water, the pipeline will float up in the later stage, as demonstrated in Fig. 4. The permanent horizontal displacement and the upward floatation of the pipeline undoubtedly cause its surrounding seabed soil deforming correspondingly, as shown in Fig. 6. It is observed that the seabed soil over the pipeline also move relatively upward to the surface layer soil of the seabed away from the pipeline, which is driven by the floating behaviour of the pipeline. It is indicated that the interaction between the pipeline and its surrounding seabed soil is intensive.

This upheaval of the seabed soil over the pipeline is also clearly observed most recently by Miyamoto et al. (2020) in their centrifuge wave flume tests, indicating again that the integrated model FSSI-CAS 2D can effectively handle the intensive nonlinear pipeline-soil interaction in computation.

In this study, the numerical computation is terminated automatically at the time  $t = 156$  s (about 20 wave periods) due to the non-convergence of numerical solving. The reasons are mainly attributed to the facts that: (1) the used soil model PZIII is a type of complicated elato-plastic soil constitutive model for loose soil, resulting in that it is not easy to keep converged state in computation; (2) the interaction between the pipeline and its surrounding loose seabed soil is complicated; (3) there is no yield and potential surface in the tensile stress space for PZIII soil model. All these factors are very easy to cause the computation becoming non-convergent at the later stage, regardless of the time step interval, the size of mesh, and the type of solver chosen for the solution of linearized equations. In this study, the computation result where the integrated model FSSI-CAS 2D terminating at  $t = 156$  s is the best one after the biggest effort by us.

5.3. Effective stresses and pore pressure

In order to comprehensively understand the interaction mechanism between the pipeline and its surrounding loose soil, it is necessary to explore the wave-induced dynamics characteristics of pore pressure and effective stress in the surrounding seabed soil. The time histories of pore pressure, effective stress and void ratio  $e$  at the four typical positions A, B, C and D are demonstrated in Figs. 7-10. It is observed that the pore pressure at the four positions all only build up slightly. Namely, the residual pore pressure in the surrounding soil is not significant. However, the oscillatory pore pressure is considerable. It is also observed that the mean effective stress  $I_1 = (\sigma'_x + \sigma'_y + \sigma'_z)/3$  all reduce from their initial values to a small magnitude (about  $-2$  kPa, noted: negative value means compressible) in the process of pore pressure slightly building up. It is worthy pointing out that there is no position where the effective stress  $I_1$  could reach zero, becoming fully liquefied. It means that only partial liquefaction could occur. This phenomenon is significantly different with the situation if there is no pipeline buried in seabed, as revealed by Yang and Ye (2017) that the loosely deposited seabed soil can become fully liquefied under wave and current loading. It is indicated that the existence of the pipeline has significant effect on the dynamics of the surrounding seabed soil.

Similarly, the time histories of the shear stress also show that the absolute value of residual shear stress at the four positions reduce, gradually approaching zero in the process of pore pressure slightly building up. The oscillatory component in the time history of the wave

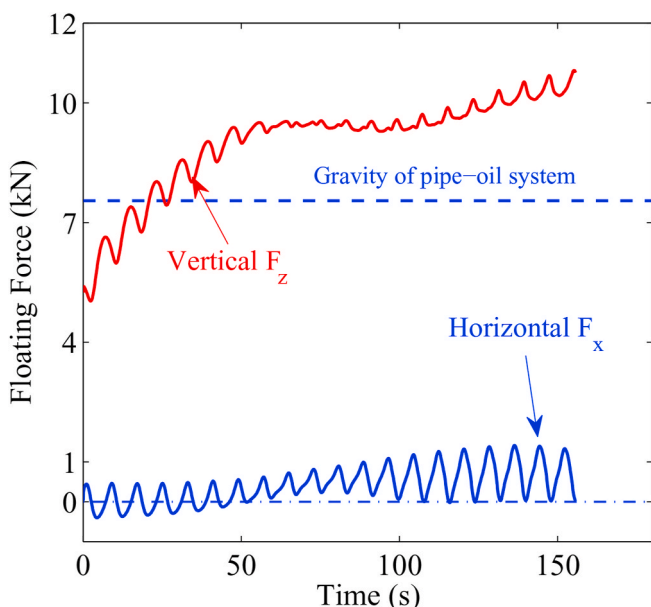


Fig. 5. Time history of the floating force applied on the pipeline.

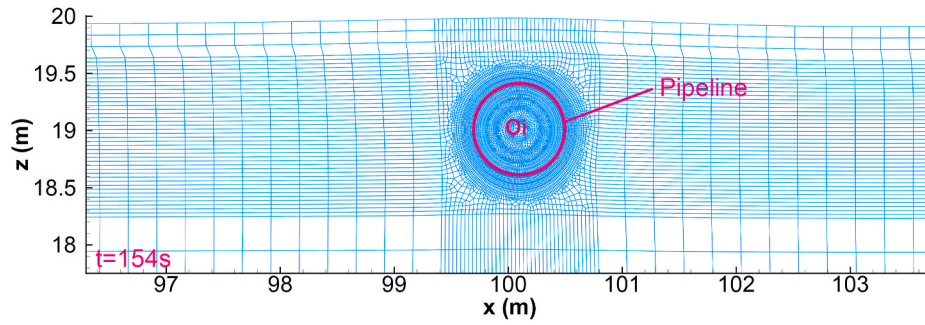


Fig. 6. Deformation of the seabed foundation surrounding the pipeline under the action of wave-current.

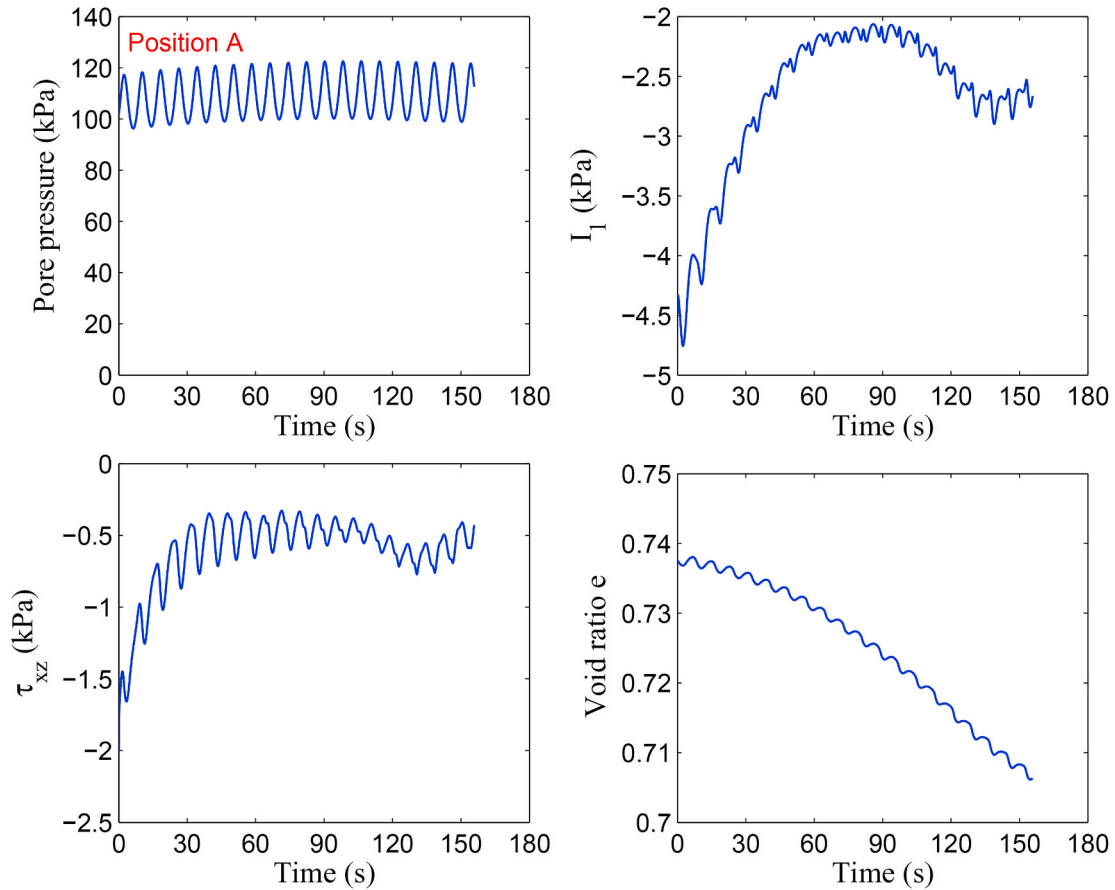


Fig. 7. Time history of the pore pressure, effective stress and void ratio at the typical position A.

and current induced shear stress also indicates that the soil at the four positions do not become fully liquefied. Otherwise, the oscillatory component should disappear as that revealed by Yang and Ye (2017), due to the fact that a fully liquefied soil behaves like a kind of heavy fluid with apparently large viscosity, without the ability to transmit shear wave and shear stress.

It is interesting to find that the void ratio of the soil at the position A and B gradually become smaller and smaller in the loading process. Meanwhile, the void ratio of the soil at the position C and D basically keep unchanged before  $t = 70$  s. After that, their void ratio increase quickly under the wave and current cyclic loading. It means that the seabed soil over the pipeline becomes denser and denser (soil permeability reduces correspondingly), meanwhile the seabed soil beneath the pipeline gradually dilates (soil permeability increases correspondingly) under cyclic loading. This phenomenon can be attributed to the upward displacement of the pipeline driven by the increasing upward floating

force applied on the pipeline, as illustrated in Fig. 5. Generally, the quick increasing of void ratio of soil would result in the quick drop of pore pressure from the perspective of linearity. However, the pore pressure at the position C and D do not drop as expected, as shown in Figs. 9 and 10. It is further indicated that the interaction between the pipeline and its surrounding loose seabed is nonlinear and complicated.

Except the time history of pore pressure and effective stress, the distribution of pore pressure and effective stress in the surrounding seabed soil around the pipeline at several typical times are shown in Fig. 11. It can be observed in Fig. 11 that the residual pore pressure doesn't build up uniformly around the pipeline. The residual pore pressure in the seabed soil beneath the pipeline is greater than that in the seabed soil over the pipeline, indicating that the rate of building up of the pore pressure beneath the pipeline is greater than that in the zone over the pipeline. It is also found that the residual pore pressure around the pipeline maximumly doesn't exceed 10 kPa.

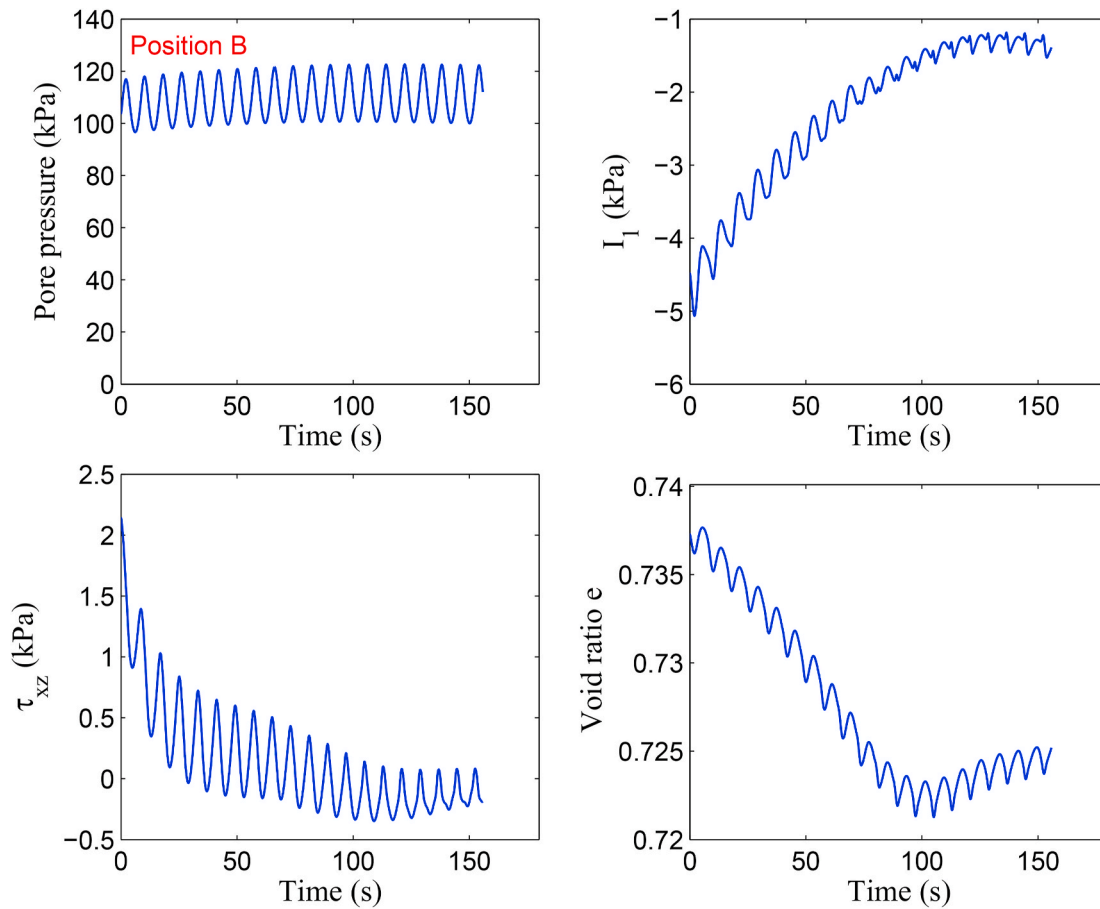


Fig. 8. Time history of the pore pressure, effective stress and void ratio at the typical position B.

At the initial state ( $t = 0s$ ), the mean effective stress  $I_1$  around the pipeline are all less than 10 kPa; and the  $I_1$  beneath the pipeline is greater than that in the zone over the pipeline, due to the gravity compression of the steel pipeline -crude oil system. After  $t = 100 s$ , the  $I_1$  around the pipeline generally is less than 2 kPa. There is no position where  $I_1$  becomes zero. It means there is no a position where the surrounding loose seabed soil becomes fully liquefied. Only partial liquefaction could be observed. Due to the existence of the pipeline, there is shear stress in the seabed soil around the pipeline at the initial time. Additionally, the shear stress around the pipeline is also not uniform. The distribution of the shear stress like a flower with four petals at the initial state. Among the four petals, the one in the range of  $210^\circ\text{--}260^\circ$  is the smallest, as demonstrated in Fig. 11. In the loading process applied by the wave and current, the shear stress in the seabed soil around the pipeline significantly reduces. Actually, the variation of this shear stress's distribution around the pipeline is very complicated, due to the complexity of the interaction between the pipeline and its surrounding loose seabed soil.

Besides the time history, it is also meaningful and necessary to explore the distribution characteristics of the wave-induced pore pressure and effective stress in the surrounding seabed soil of the pipeline. As illustrated in Fig. 12, the distribution of pore pressure at  $t = 150 s$  is not strictly layered any more due to the uneven accumulation of pore pressure in the seabed. However, the distorted effect on the layered distribution of the pore pressure is very limited because the magnitude of pore pressure accumulation is not significant in the upper seabed, as demonstrated in Figs. 7–10. Due to the fact that the steel pipeline is not porous, the pore pressure inside and outside of the steel pipeline is isolated. The pressure inside of the pipeline keeps as 200 kPa, which is not affected by the pore pressure build up in the surrounding seabed soil.

In the process of pore pressure build up, the effective stress in seabed will certainly reduce if there is no buried pipeline (Yang and Ye, 2018). However, the existence of the pipeline makes the distribution of the mean effective stress  $I_1$  in the surrounding seabed of the pipeline much more complicated. Overall,  $I_1$  is all reduced relative to their initial value except in some local zone over the pipeline, in which the  $I_1$  is greater than its initial value. This is due to the fact that the seabed soil over the pipeline is extruded by the upward floating pipeline driven by the accumulated residual pore pressure in the surrounding seabed soil. In the zone away from the pipeline, the distribution of  $I_1$  is almost layered, as that demonstrated by Yang and Ye (2018) where there is no buried pipeline. In the upper seabed ( $z = 18\text{ m--}20\text{ m}$ ) away from the pipeline, the magnitude of  $I_1$  generally is less than 1 kPa, indicating that the seabed soil in this zone becomes liquefied with high possibility. In the surrounding seabed soil of the pipeline, the effect of the pipeline is very significant. The  $I_1$  in this zone generally is greater than 1 kPa, indicating that the seabed soil in this zone is not likely to liquefy. Additionally, it is observed that there is a small zone with high magnitude of effective stress over the pipeline, where the mean effective stress  $I_1$  is much greater than that in its near zone. This is also due to the upward floating of the pipeline. Exactly due to the gravity effect, the  $I_1$  in the zone beneath the pipeline is significantly greater than that in the counterpart zone in the seabed.

The distribution of shear stress at  $t = 150 s$  is significantly different with its initial symmetrical distribution. There is no any characteristics of symmetry, and the maximum magnitude of the shear stress in the surrounding seabed soil of the pipeline is only 1 kPa, which is much less than that in the initial state. In the zone away from the pipeline, the magnitude of shear stress is all near to zero. This phenomenon further indicates that the seabed soil away from the pipeline is likely to become

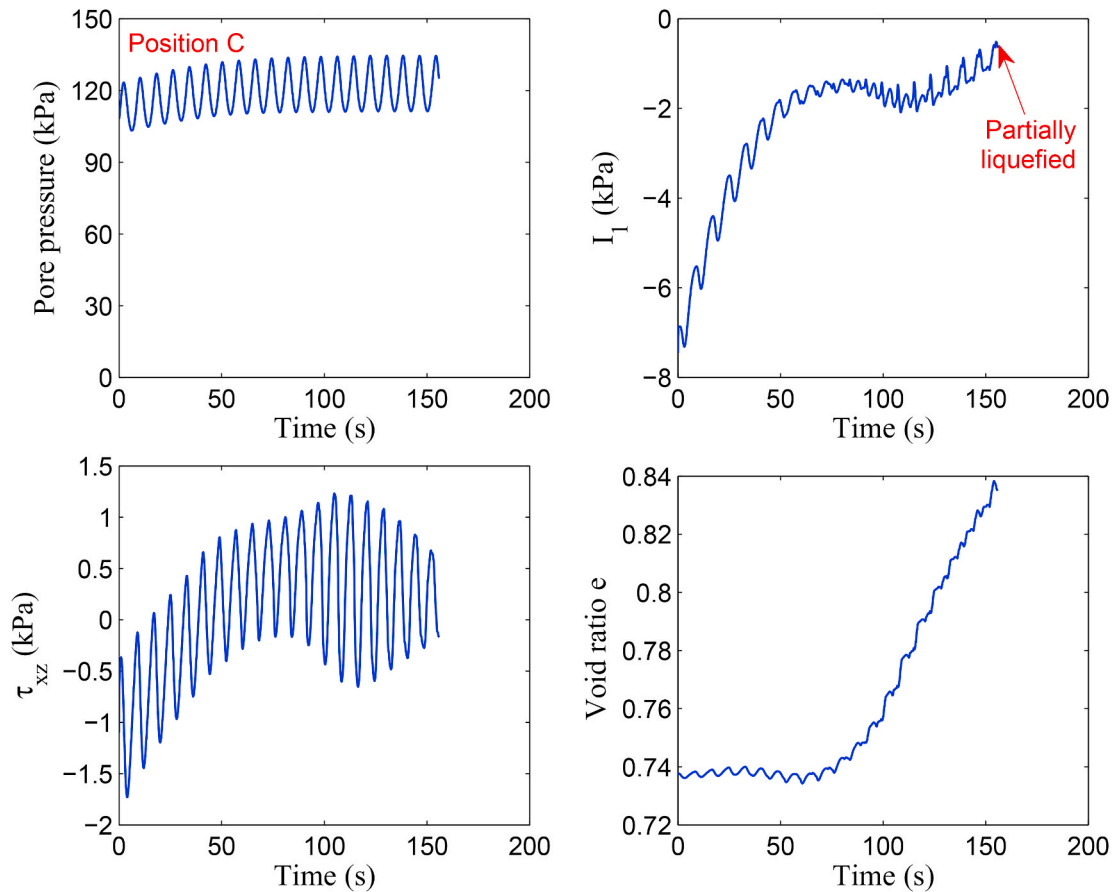


Fig. 9. Time history of the pore pressure, effective stress and void ratio at the typical position C.

liquefied, while the surrounding seabed soil of the pipeline is not likely to become liquefied at the end of computation.

Fig. 13 illustrates the relation between the shear stress and shear strain at the four typical position A, B, C and D around the pipeline. It is found that the direction of shear strain at position A, C is opposite with that at position B, D. To the end of computation, the magnitude of shear strain at the four positions is in the range of 6%–13%, and the magnitude of shear strain at position C and D beneath the pipeline is greater than that on the position A and B which is over the pipeline. On the position A and B, the magnitude of the residual shear strain gradually reduces respectively to about 500 Pa and 0 Pa, with the pore pressure build up induced by wave & current loading. On position C and D, the shear strain is very small at early time until the occurrence of stiffness softening of seabed soil. After that, a significant cyclic mobilization is observed. Due to the fact that the amplitude of the cyclic mobilization is in the range of 500–1200 Pa, the seabed soil on the position C and D is not likely to become liquefied at  $t = 150$ s, This conclusion is consistent with that obtained from Fig. 12.

#### 5.4. Liquefaction

It has been widely proved that loosely deposited seabed soil could become liquefied under continuous hydrodynamic loading by laboratory tests (Sassa and Sekiguchi, 1999) and field records (Sassa et al., 2006). Generally, there are two types of liquefaction mechanisms for seabed soil. The first one is the momentary liquefaction which could only occur in very dense sandy soil under wave trough due to the upward seepage force. Its effect on the stability of offshore structures is not significant. However, the momentary liquefaction could significantly boost the scouring of seabed soil around offshore structures. Another one is the residual liquefaction occurring due to the pore pressure

accumulation in loosely deposited soil under cyclic loading. The liquefaction occurring in the loosely deposited seabed soil in this study is exactly the residual liquefaction. Generally, residual liquefaction in loose seabed foundation has adverse effect on the stability of offshore structures. Once residual liquefaction occurs in seabed soil, the bearing capacity of seabed soil will significantly lost, which could result in a series of engineering failures, e.g., the upheaval bulking and the breaking of offshore pipeline.

Generally, there are two kinds of criteria to quantitatively access and judge the occurrence of residual liquefaction in loose seabed soil (Yang and Ye, 2018). The first one is the pore pressure-based criteria. This kind of criterion defines a ratio between excess pore pressure and initial effective stress. When this ratio is greater than a critical value, e.g. 0.8, residual liquefaction is judged to occur for seabed soil. As pointed by Ye and Wang (2015), this pore pressure-based criteria can only be used for the cases in which there is no offshore structure involved. If an offshore structure is built on or buried in seabed foundation, then the pore pressure-based criteria is actually not a reliable criteria to judge the occurrence of residual liquefaction due to the fact that there probably is intensive soil-structure interaction. Ye and Wang (2015) presented a reliable case to demonstrate this conclusion, in which a large scale offshore breakwater was built on a loosely deposited seabed foundation. Their results showed that the breakwater subsided about 5 m and laterally moved to one side about 12 m under the attacking of a seismic wave. In the process, the pore pressure significantly built up exceeding its initial effective stress, meanwhile the effective stress gradually increased however, rather than reduced in the seabed soil beneath the breakwater caused by the large deformation of seabed foundation, as well as the great subsidence and tilting of the overlying breakwater. Ye and Wang (2015) also presented an interesting result that the residual pore pressure reached up to double times of the initial effective stress

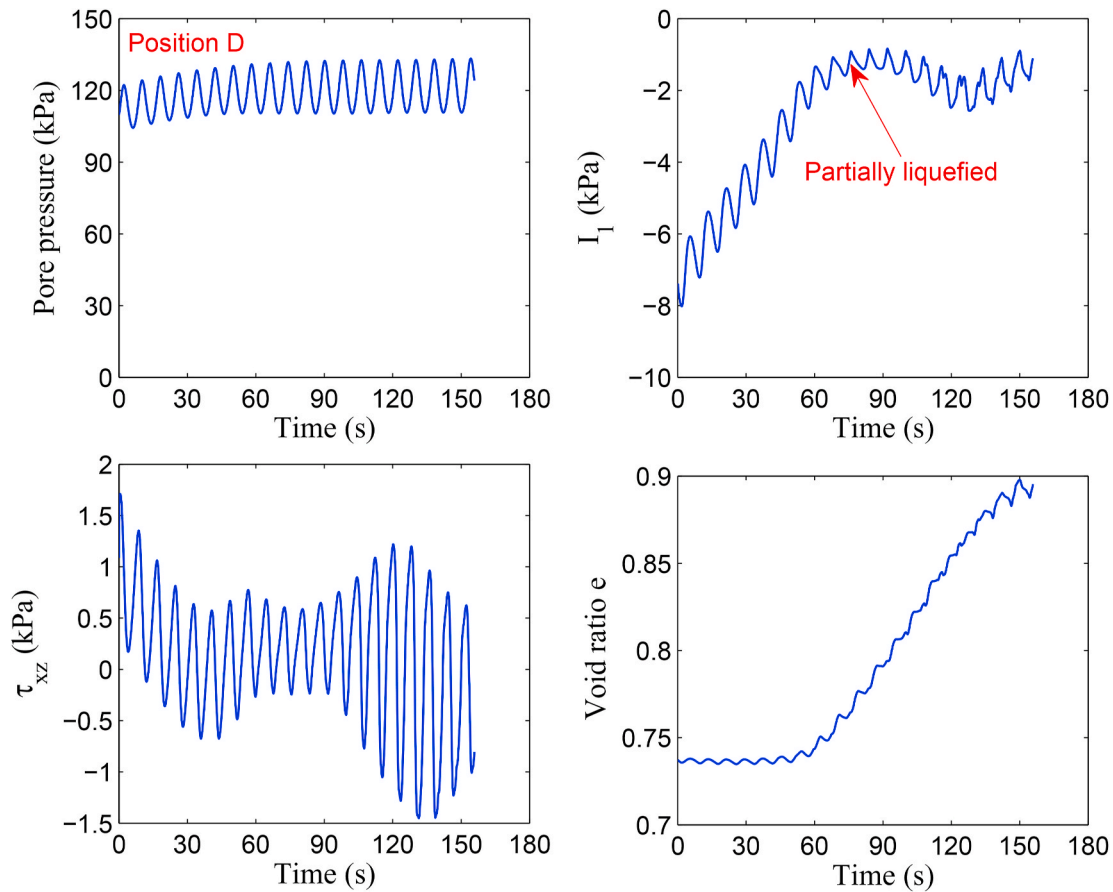


Fig. 10. Time history of the pore pressure, effective stress and void ratio at the typical position D.

when the seabed soil becoming fully liquefied at a position. Based on previous conventional recognition, the residual pore pressure in sandy seabed soil (cohesion is zero) is impossible to be greater than the corresponding initial effective stress if there is no offshore structure. Exactly due to the presence of the offshore breakwater, as well as the intensive soil-structure interaction, the development of residual pore pressure and effective stress in seabed foundation is highly complex. The pore pressure-based criteria actually is an indirect judgement criterion. It is not suggested to be used in the cases where soil-structure interaction is involved.

The second method is based on the effective stress. According to the traditional definition of soil liquefaction, the most obvious physical characteristics of soil liquefaction is that the effective stress between soil particles approaches to zero (partial liquefaction) or exactly is equal to zero (fully liquefaction). Therefore, we can adopt this physical characteristics to judge the occurrence of soil liquefaction. As a result, the effective stress-based criterion is a type of direct criteria. Based on this recognition, two specific formulations have been proposed by the authors in previous literatures (Ye and Wang, 2015; Yang and Ye, 2018) to access the residual liquefaction of loose seabed soil. The first one is that a parameter referred as to residual liquefaction potential  $L_p$  is defined to describe the liquefaction potential of loose seabed soil under cyclic loading (Noted: compressive stress is taken as negative value):

$$L_p = \frac{\sigma'_{zd}}{-\sigma'_{z0} + \alpha c} \geq (L_p)_{critical} \quad (8)$$

where  $\sigma'_{zd} = \sigma'_z - \sigma'_{z0}$  is wave-induced dynamic vertical effective stress;  $\sigma'_{z0}$  is initial vertical effective stress;  $\sigma'_z$  is current vertical effective stress.  $c$  is cohesion of seabed soil;  $\alpha$  is a dimensionless material coefficient. In Equation (8), the cohesion of seabed soil is taken into

consideration. From the perspective of that it is much more difficult for cohesive soil to become liquefied under cyclic loading, cohesion of soil could effectively enhance the liquefaction resistance of soil  $L_r = -\sigma'_{z0} + \alpha c$  (Liu and Jeng, 2016). Therefore, it is better to consider the cohesion  $c$  of soil when evaluate liquefaction potential. More detailed explanation on  $\alpha$  and soil cohesion is available in Yang and Ye (2018). In this study, cohesion  $c$  is zero because seabed is assumed as sandy soil. Then, there is no effect of  $\alpha$  on the  $L_p$  of sandy seabed soil. For sandy seabed soil, the residual liquefaction potential can be expressed as  $L_p = 1 - \frac{\sigma'_z}{\sigma'_{z0}}$ . If the effective stresses in 3D situation are considered, it becomes  $L_p = 1 - \frac{I_1}{(I_1)_0}$ , where  $(I_1)_0$  is the initial mean effective stress.  $(L_p)_{critical}$  is a critical value given by engineers and scientists involved. When  $L_p$  is greater than or equal to the given  $(L_p)_{critical}$  at a position, the seabed soil at this position can be judged to become liquefied. On the issue of the value range of  $L_p$ , generally it is in the range of 0.0–1.0. In the case of intensive soil-structure nonlinear interaction,  $L_p$  in some local zones could be less than 0.0 due to the fact that  $|\sigma'_z|$  could be greater than  $|\sigma'_{z0}|$ , even through the pore pressure has been significantly built up, as the results presented in Ye and Wang (2015).

The second judgement formulation of the effective stress-based criteria is  $|I_1| \leq (I_1)_{critical}$ , where  $(I_1)_{critical}$  is also a critical value given by engineers and scientists involved. It means that the residual liquefaction will occur at a position where if the current mean effective stress  $|I_1|$  is less than or equal to the given critical value  $(I_1)_{critical}$ . Due to the fact that sandy soil can not bear any tensile stress, the mean effective stress  $I_1$  in sandy seabed soil must be negative. Generally, the critical value  $(I_1)_{critical}$  given by engineers and scientists is a small value close to zero, e.g. 1 kPa. In theory, the current  $|I_1|$  must be very small in partially liquefied situation, or must be equal to zero in fully liquefied situation. Therefore, this effective stress-based judgement formulation for soil

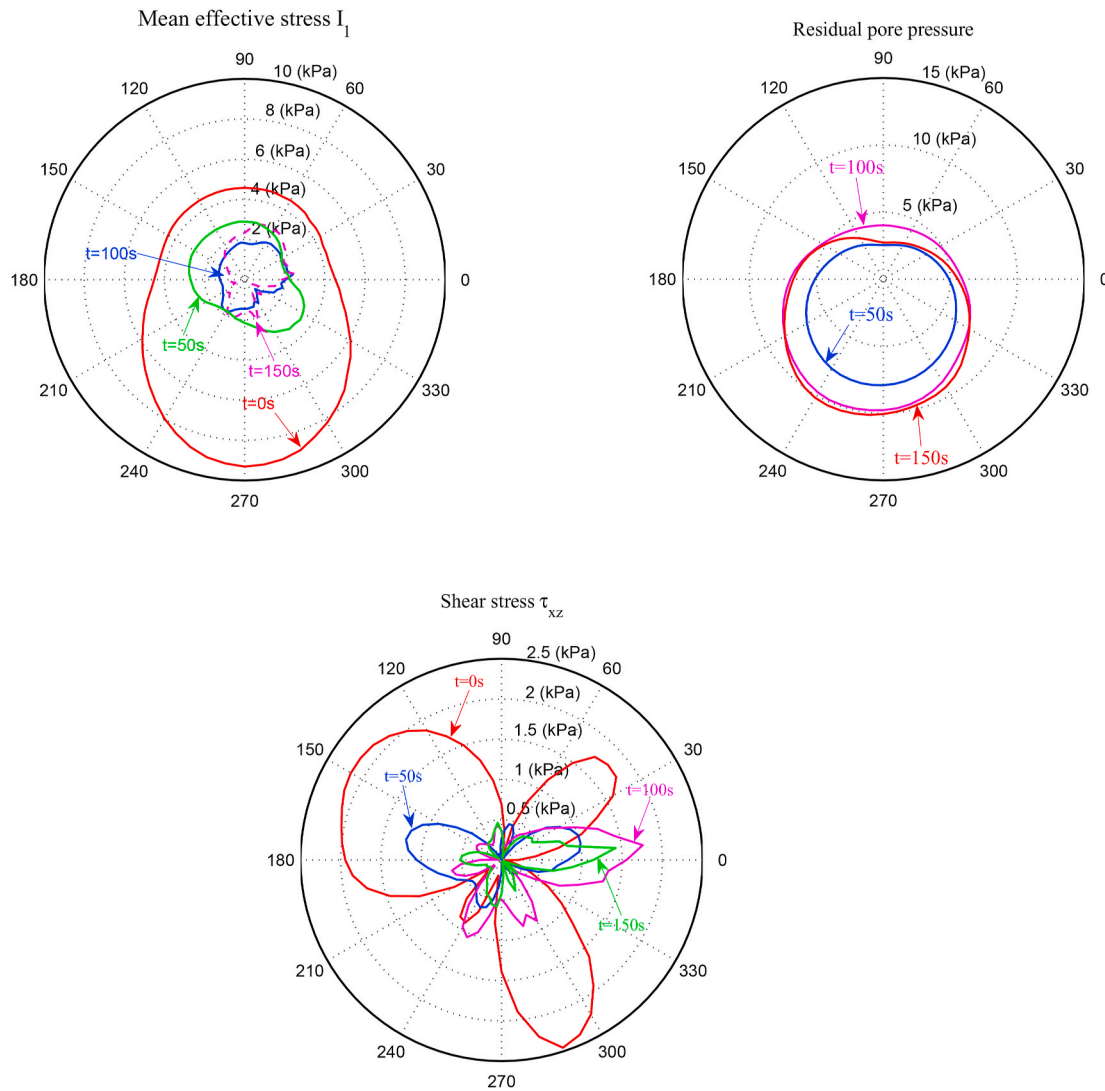


Fig. 11. Development of the pore pressure and effective stress in the surrounding seabed soil of the pipeline.

liquefaction adopting the current  $|I_1|$  is more in line with the definition of liquefaction than that of  $L_p$ .

Although Equation (8) and the formulation  $|I_1| \leq (I_1)_{critical}$  are both the effective stress-based criterion for soil residual liquefaction, none of them are perfect. They each have their own strengths and weaknesses. For the first judgement formulation (Equation (8)), the value of  $\alpha$  currently is impossible to be quantitatively determined in terms of experiments or theoretic analysis because very little attention has been paid on it by scholars. Therefore, the first judgement formulation is not applicable for clay and silty soil. Additionally, the critical value  $(L_p)_{critical}$  is not a constant value for all types of soils, but need to be given by engineers or scientists based on their engineering experiences and theoretic analysis. As a result, unexpected artificial error would be brought. According to the suggestion of Wu et al. (2004),  $(L_p)_{critical}$  is in the range of 0.78–0.99, depending on the soil types. Previous investigation conducted by Ye et al. (2015) indicated that  $(L_p)_{critical} = 0.86$  for Nevada sand. This value will be adopted to judge the occurrence of residual liquefaction in the surrounding seabed soil of the pipeline. For the second judgement formulation, unexpected artificial error is also unavoidable when determining the critical value  $(I_1)_{critical}$ , for example, the size and shape of the predicted residual liquefaction zone would be significantly different when  $(I_1)_{critical} = 1$  kPa or  $(I_1)_{critical} = 2$  kPa. Another defect of the second judgement formulation is that it is not applicable to judge the liquefaction or not for the upper seabed soil with

shallow buried depth, e.g., the absolute mean effective stress  $|I_1|$  is certainly less than 1 kPa for the seabed soil with a buried depth less than 5 cm (near to seabed surface) at the initial state, as a result, the seabed soil will be wrongly judged to become liquefied all the time if we take  $(I_1)_{critical} = 1$  kPa, even though there would be no a wave loading on the seabed surface. However, the second judgement formulation has huge advantages to judge the occurrence of liquefaction for the seabed soil which has a great initial effective stress, e.g. 100 kPa.

The distribution of the wave & current induced liquefaction zone predicted by adopting the two effective stress-based criteria at time  $t = 150$  s are shown in Figs. 14 and 15. In Fig. 14, the critical  $L_p$  is set as 0.86 following the suggestion of Ye et al. (2015). It is observed that the upper seabed soil with shallow buried depth away from the pipeline all becomes liquefied with a liquefaction depth about 1.0–2.0 m. Meanwhile, the seabed soil surrounding the pipeline is all not liquefied. It is indicated that the presence of the pipeline indeed has significant effect on the wave-induced dynamics of its surrounding seabed soil. It is worth to point out that the seabed soil over the pipeline is also not liquefied, even though this part of seabed soil is directly applied by the wave & current hydrodynamic loading. This phenomenon is attributed to that the upward floating of the pipeline brings extrusion effect to the seabed soil over the pipeline, making the effective stress in it is compressive with a great magnitude. This high stress zone over the pipeline actually can be clearly observed in the  $I_1$  distribution in Fig. 12. Even though the  $L_p$  in

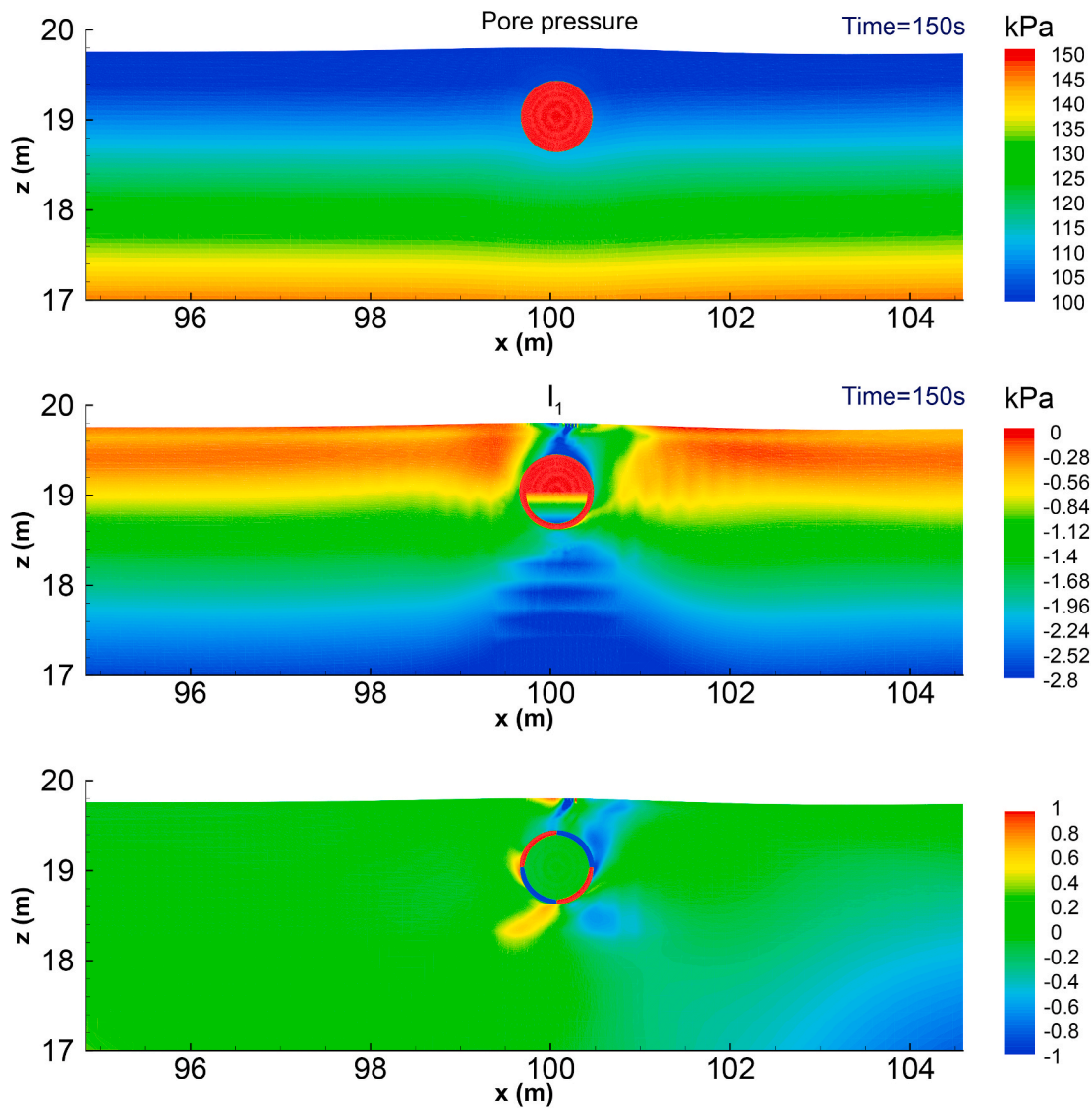


Fig. 12. Distribution of the pressure and effective stress in the seabed foundation at time  $t = 150$  s.

the surrounding seabed soil of the pipeline does not exceed the set critical value 0.86 (liquefaction does not occur), it does not mean that the stiffness of the surrounding seabed soil not to attenuate. Actually, softening is always occurring in the surrounding seabed soil of the pipeline accompanying the accumulation of pore pressure and reduction of effective stress. The interaction between the pipeline and its surrounding seabed soil must be properly considered in computation. Otherwise, the computational results is not reliable and convincing, or even wrong.

There is no unified standard for the artificial selection of the value of  $(I_1)_{critical}$  in the domain of offshore geotechnics so far. As stated above, the size and the shape of the predicted liquefaction zone will largely depend on the selected value of  $(I_1)_{critical}$ . In theory, soil can become fully liquefied only when the  $I_1$  reduces to zero from a great initial value. However, it is difficult for seabed soil to reach this extreme state in which  $I_1 = 0$  kPa. Actually, large deformation in seabed foundation would have occurred before  $I_1$  approaching zero, presenting the liquefaction characteristics of soil. Under this situation, liquefaction is deemed has been occurred in the perspective of engineering practices. Therefore, the value of  $(I_1)_{critical}$  absolutely can not be set as zero. Otherwise, there would be on liquefaction occurs in seabed foundation under any hydrodynamic loading. On the other hand, the reasonable

selection of the value of  $(I_1)_{critical}$  decided by engineers and scientists needs based on the engineering experiences and experimental data together. In this study, we set the value of  $(I_1)_{critical}$  as 1.0 kPa to predict the liquefaction zone distribution near to the pipeline, as shown in Fig. 15. It is observed that the distribution of the liquefaction zone predicted adopting  $|I_1|$  is similar with that predicted adopting  $L_p$ . The only differences include: (1) the liquefaction depth is about the 1.2 m, which is much less that in Fig. 14; (2) the area of the non-liquefied zone surrounding the pipeline is significantly smaller than that predicted adopting  $L_p$ . It is indicated that the effective stress-based criteria adopting  $L_p$  and  $|I_1|$  are both acceptable to predict the liquefaction zone surrounding the pipeline, even though there is intensive soil-structure interaction.

### 5.5. Effect of the pipeline-gas system

In the practice of engineering, marine pipeline is not only used to transport crude oil, but also natural gas (density is  $0.7174 \text{ kg/m}^3$  at 1 atm pressure). In this study, the wave & current-induced dynamics of the pipeline-gas system buried in the same loosely deposited seabed foundation is also investigated, to seek the differences of dynamics between the pipeline-oil system and the pipeline-gas system applied by

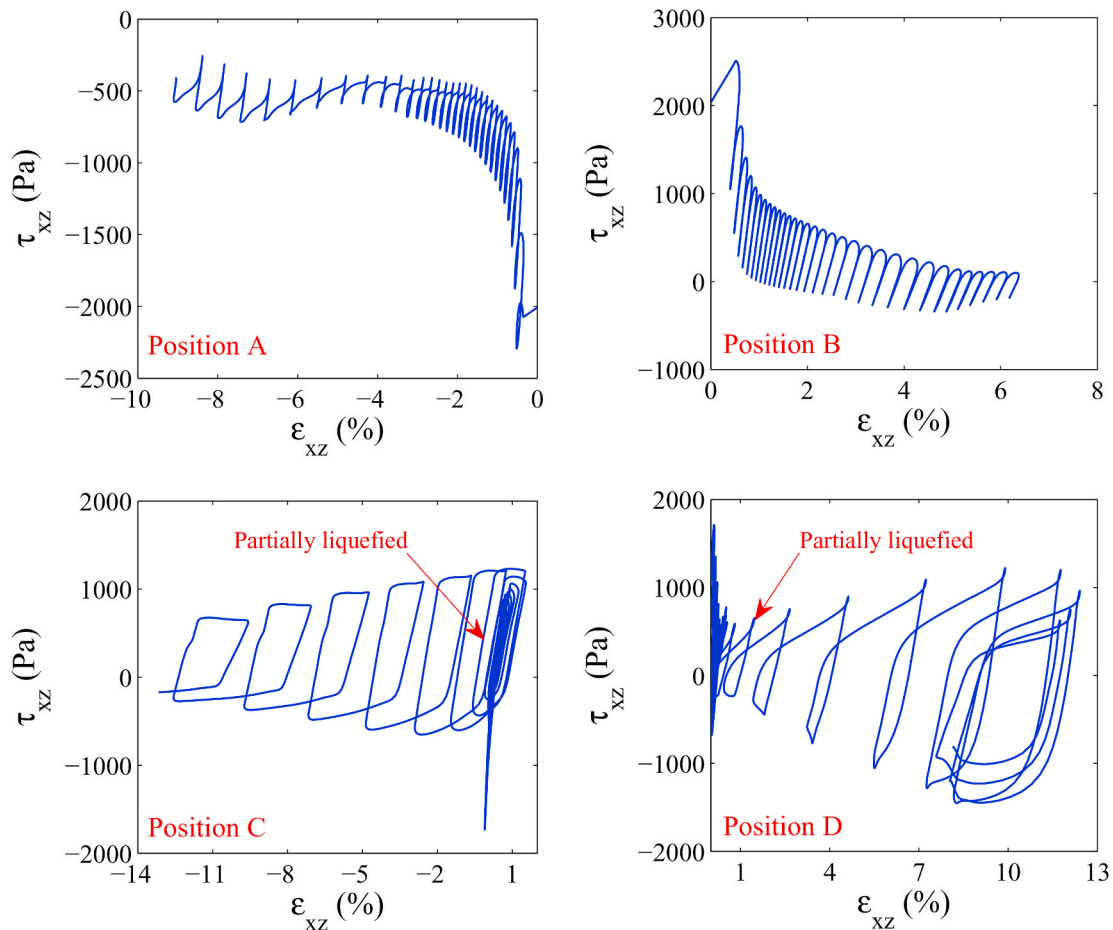


Fig. 13. Stress-strain relationship at the four typical positions.

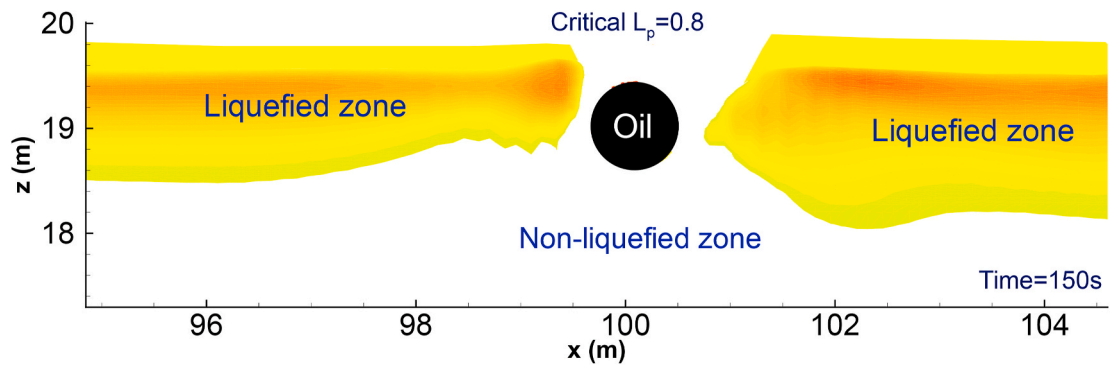


Fig. 14. Liquefaction zone in the region near to the pipeline predicted by adopting  $L_{potentia}$  (the first effective stress-based criterion).

hydrodynamic loading.

Firstly, the distribution of displacements, pore pressure and effective stresses of the pipeline-gas-seabed system at the initial state, as have been shown in Figs. 16 and 17, are compared with that of the pipeline-oil-seabed system. In Fig. 16, it is found that the distribution of the initial displacement is completely different with that if crude oil is transported in the pipeline. In the case crude oil is transported, the downward subsidence of the pipeline at the initial state is about 28.2 mm, which is more than the subsidence of its surrounding seabed soil (see Fig. 4 in Zhang et al. (2019)). It means that the pipeline-oil system slightly sinks downward relative to its surrounding soil caused by the considerable weight of the pipeline-oil system. Oppositely, the downward subsidence of the pipeline is only 27 mm, which is less than the subsidence of its

surrounding seabed soil, as illustrated in Fig. 16. It means that the pipeline-gas system slightly floats upward relative to its surrounding soil. Of course, this phenomenon is due to that the density of natural gas is much less than that of crude oil. The weight of the pipeline-gas system is certainly less than that of pipeline-oil system. However, the buoyancy applied by the hydrostatic water pressure on the steel pipeline is the same due to the fact that the volume of pore water expelled by the pipeline has no change. As a result, the pipeline-gas system certainly will have a strong trend to float upward even at the initial state. Exactly because of this upward floating trend of the pipeline-gas system, the low stress zone beneath the pipeline is larger in size than that if crude oil is transported (see Fig. 5 in Zhang et al. (2019)), as demonstrated in Fig. 17. Also due to this slight sinking and slight floating of the pipeline

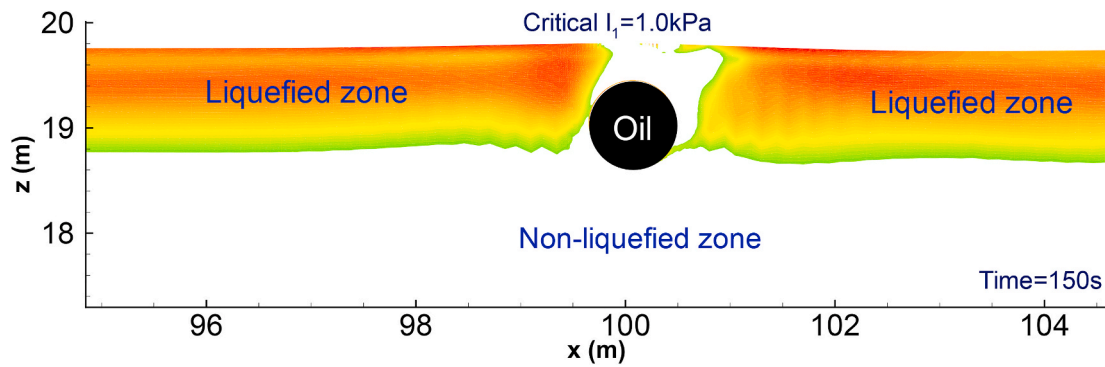


Fig. 15. Liquefaction zone in the region near to the pipeline predicted by adopting  $|I_1|$  (the second effective stress-based criterion).

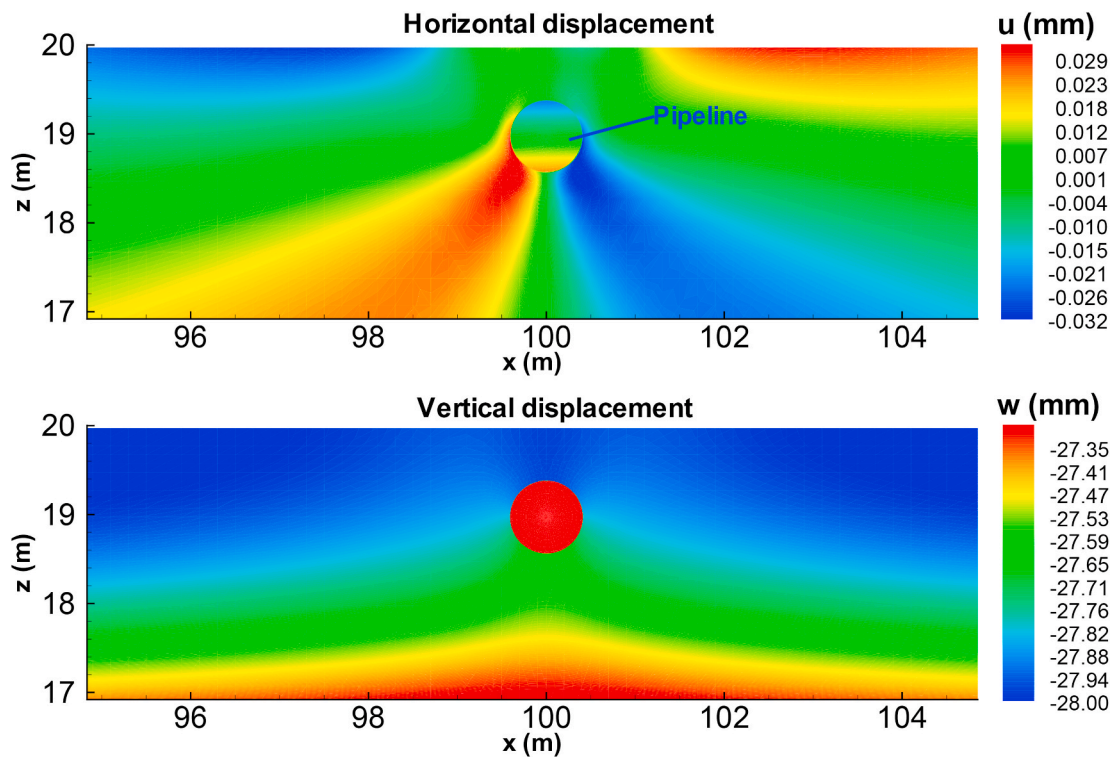


Fig. 16. Distribution of the displacement at the initial state when natural gas is transported by the pipeline.

relative to its surrounding seabed soil, the distribution of the initial horizontal displacement around the pipeline is significantly different. However, they both have symmetry along  $x = 100$  m. Similarly, it is observed in Fig. 17 that the distribution of pore pressure in the seabed is also layered without any excess pore pressure. The distribution of the initial shear stress  $\tau_{xz}$  around the pipeline shown in Fig. 17 is also different with the distribution where crude oil is transported. The domain of influence of  $\tau_{xz}$  beneath the pipeline is obviously larger than that over the pipeline. Nevertheless, the domain of influence of the initial  $\tau_{xz}$  beneath and over the pipeline basically is same for pipeline-oil system. This difference is also caused by the slight sinking and slight floating of the pipeline relative to its surrounding seabed soil at the initial state.

The comparison of the time history of the wave & current-induced displacement of the pipeline is illustrated in Fig. 18. It is observed that the difference of the horizontal displacement of the pipeline is minor. However, the difference of the vertical displacement is significant between the pipeline-oil system and the pipeline-gas system. Whether it is crude oil or natural gas transported, the pipeline firstly sinks relative to

its initial position under hydrodynamic loading in the early stage until to the moment when the upward buoyancy applied on the pipeline become greater than the gravity of the pipeline-oil/gas system. After that, the pipeline will gradually float up. To the end of computation, the pipeline transporting natural gas floats up about 100 mm relative to its initial position, which is much greater than that of the pipeline transporting crude oil (about 25 mm). As illustrated in Fig. 19, the difference of the upward buoyancy applied on the pipeline by the wave & current-induced excess pore pressure is not very significant. However, the gravity of the pipeline-gas system is much less than that of the pipeline-oil system. As a result, the pipeline transporting natural gas certainly will float up much more. This substantial floating of the pipeline-gas system with a magnitude of 100 mm will extrude the seabed soil over the pipeline with a more obvious way, making the seabed over the pipeline hunch more significantly than that if crude oil is transported, as that demonstrated in Fig. 20. It is worth to point out that a pipeline could float up to the surface and finally seating on seabed. This penetration process of the pipeline actually is very difficult to be numerically modelled due to the fact the FE method is not good at handling such

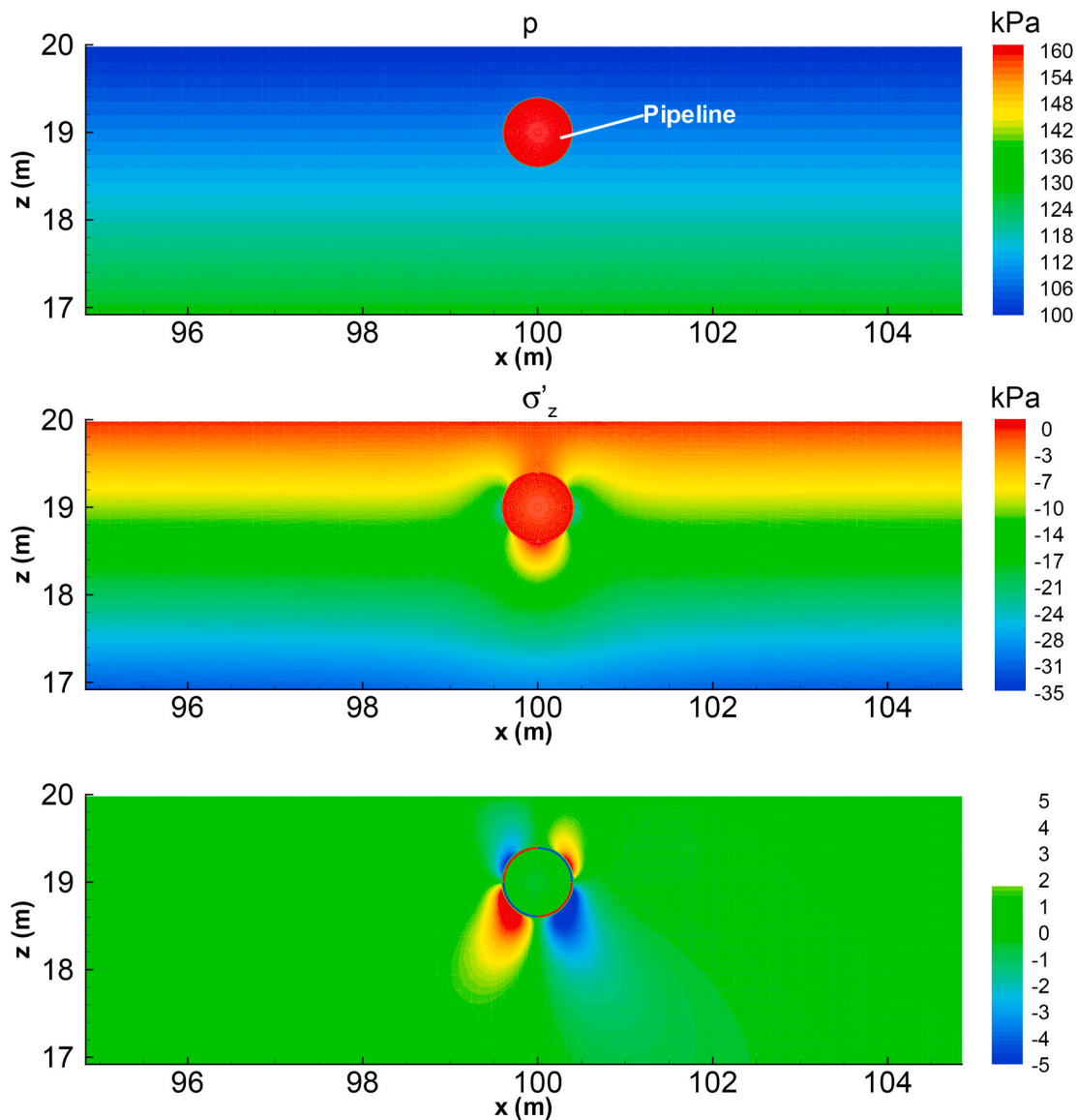


Fig. 17. Distribution of the pressure and effective stress at the initial state when natural gas is transported by the pipeline.

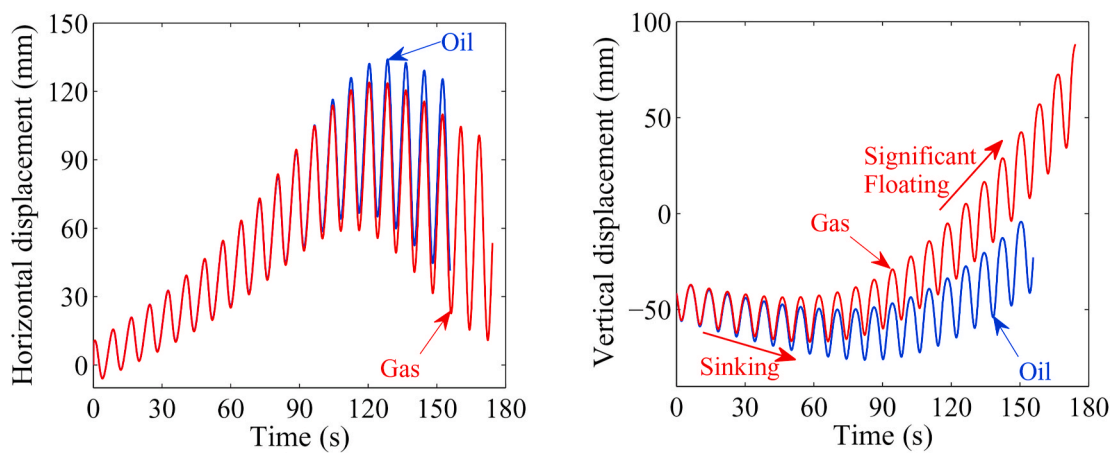


Fig. 18. Comparison of the time history of the pipeline's displacement induced by wave-current in the cases where crude oil or natural gas is transported.

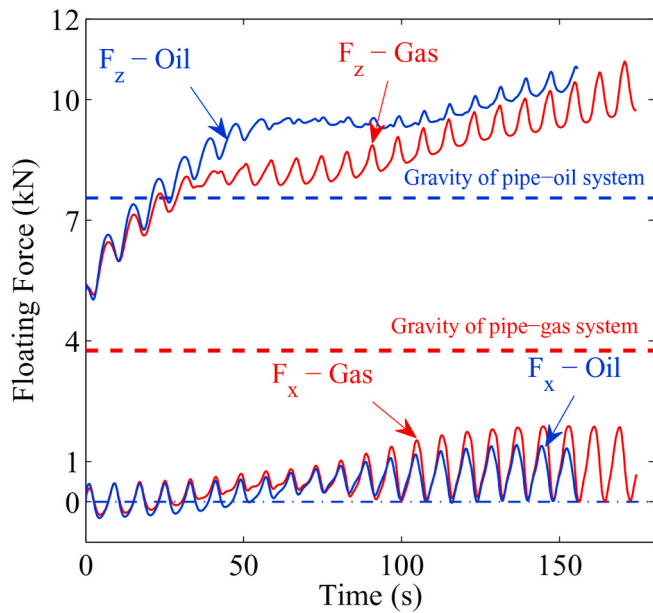


Fig. 19. Comparison of the wave-current induced buoyancy applied on the pipeline in the cases where crude oil or natural gas is transported.

great distortion of mesh adopting ALE method. Although CEL method could handle large deformation problems to some extends, the complicated fluid-solid interaction, structure-soil interaction, as well as nonlinear dynamic behaviours can not be effectively handled by CEL method.

Fig. 21 illustrates the time history comparison of the wave & current-induced pore pressure, effective stress and void ratio at the typical position D. It is found that the time history of the pore pressure and shear stress basically is the same for the pipeline-oil/gas systems. Due to the greater gravity of the pipeline-oil system, the initial mean effective stress  $|I_1|$  at the position D under the pipeline is greater than that if natural gas is transported. In addition to this point, there is no essential difference on the time history of  $I_1$ . The most significant difference is presented on the time history of void ratio. At the position D under the pipeline, the seabed soil dilates very significantly regardless of crude oil or natural gas being transported accompanying the floating up of the pipeline. However, the magnitude of dilation of the seabed soil under the pipeline transporting natural gas is much greater than that if crude oil is transported. This phenomenon is attributed to the much more greater magnitude of the upward floating of the pipeline transporting natural gas, as analyzed above.

It is indispensable to compare the distribution of liquefaction zone in the seabed soil around the pipeline in which crude oil or natural gas is transported. Fig. 22 shows the liquefaction zone predicted by adopting

$|I_1|$  (the second effective stress-based criterion). It is observed that the liquefaction zone around the pipeline-gas system basically is the same with that illustrated in Fig. 15. Only the upper seabed soil with a thickness about 1.4 m away from the pipeline-gas system becomes liquefied, the seabed soil around the pipeline-gas system is also not liquefied. Overall, the biggest difference on the dynamics of the pipeline and its surrounding seabed soil between the pipeline-gas system and the pipeline-oil system is reflected on the upward floating of the pipeline driven by the excess pore pressure induced by hydrodynamic loading.

5.6. Post densification

Once the hydrodynamic loading stopping to apply, the accumulated excess pore pressure in seabed soil will gradually dissipate accompanying the gradual drainage of pore water out of seabed through the seabed surface. In this process, the effective stress in seabed soil will increase correspondingly, and the offshore structures built on or buried in seabed foundation will also correspondingly subside. Finally, the seabed foundation soil will become more dense, and get higher bearing capacity once the excess pore pressure is completely dissipated. Fig. 23 demonstrates the post densification process of the pore pressure dissipation, effective stress growth, as well as the subsidence of the pipeline transporting crude oil or natural gas. It is observed that the pore pressure indeed gradually dissipates, and the effective stress gradually grows in the surrounding seabed soil of the pipeline. The pipeline indeed gradually subsides downward after the wave & current stopping to apply hydrodynamic loading. This post densification process of the pipeline-oil/gas-seabed system is an important result for the problem of offshore pipeline dynamics due to the fact there is no attention has been paid on the issue in previous literature. It will promote us to further understand the mechanism and dynamics characteristics of offshore pipeline subjected to ocean wave hydrodynamic loading.

6. Conclusion

In this study, the dynamics of a pipeline transporting crude oil or natural gas shallowly buried in loosely deposited seabed foundation under third-order ocean wave & current loading is numerically investigated adopting the integrated model FSSI-CAS 2D, which was firstly developed by Jeng et al. (2013) and Ye et al. (2013b) specially for the problem of fluid-structure-seabed foundation interaction. Through comprehensive analysis for the computational results, the following recognitions are obtained:

- (1) The pore pressure in the surrounding seabed soil of the shallowly buried pipeline does not accumulate significantly. However, the effective stress reduces about 50%–80% relative to its initial value. It is indicated that stiffness softening has occurred in the surrounding seabed soil of the pipeline This softening provides

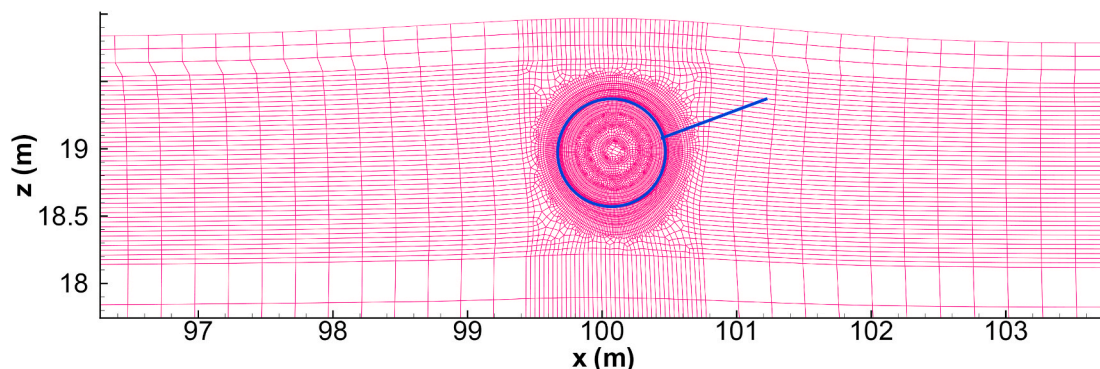


Fig. 20. Deformation of seabed foundation induced by the wave-current if natural gas is transported by the pipeline.

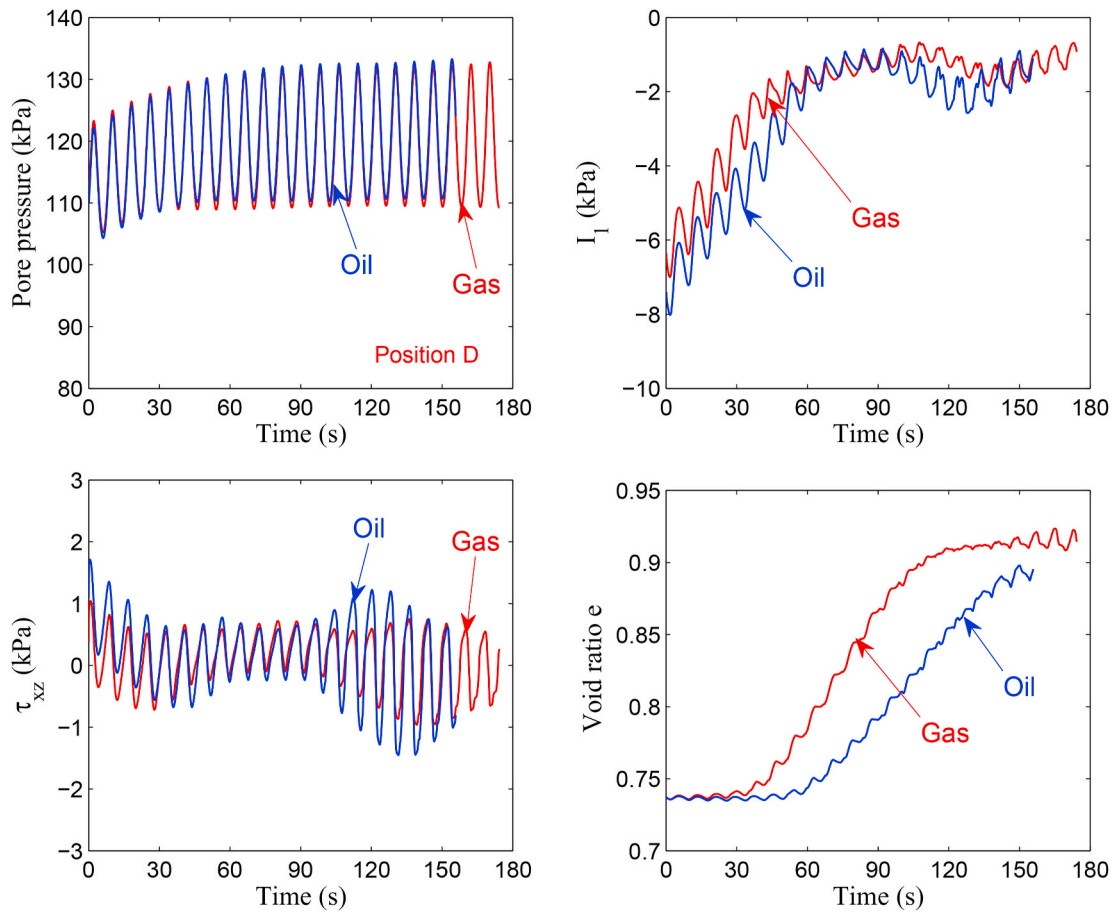


Fig. 21. Comparison of the time history of the pore pressure, effective stress and void ratio  $e$  at the position D where crude oil or natural gas is transported by the pipeline.

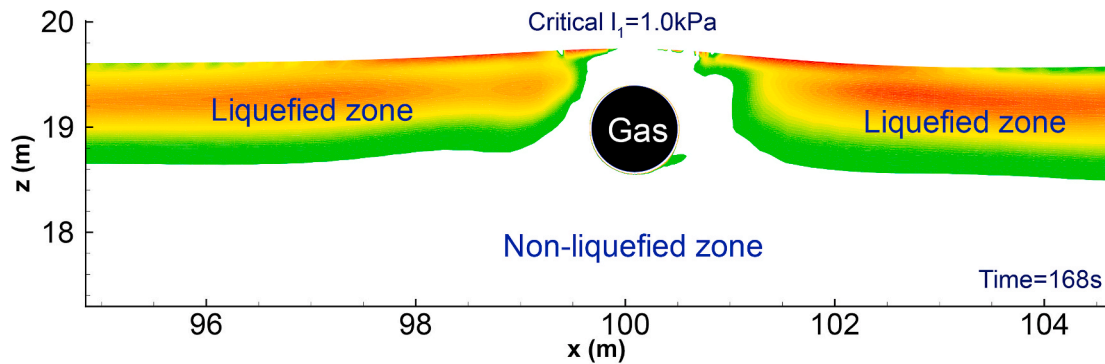
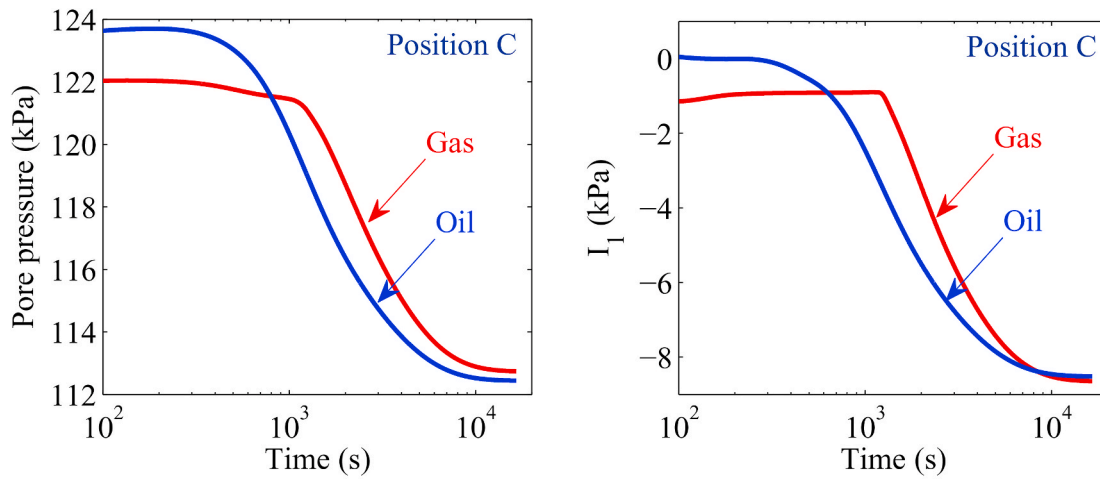


Fig. 22. Liquefaction one in the seabed soil surrounding the pipeline if natural gas is transported predicted by adopting  $|I_1|$  (the second effective stress-based criterion).

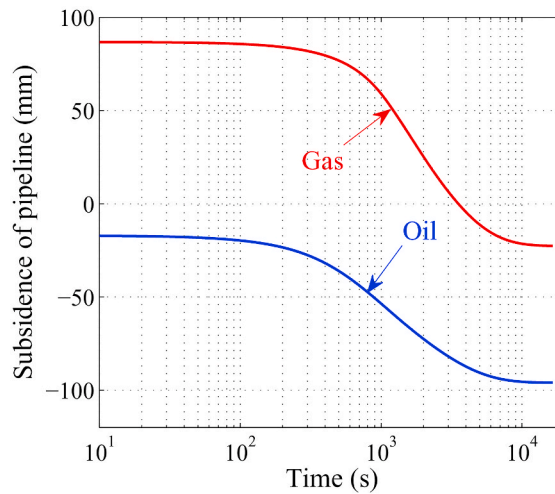
extremely favorable conditions for the horizontal, vertical vibrations, and the upward floating of pipeline. The significant floating up of the pipeline results in the occurrence of large deformation in the surrounding seabed soil. The soil over the pipeline gradually becomes denser, meanwhile the soil beneath the pipeline significantly dilates accompanying the upward floating of the pipeline.

- (2) The buoyancy applied on the pipeline is not a constant, but is gradually increased under continuous hydrodynamic loading. The increase of the buoyancy is attributed to the accumulation of the pore pressure in the surrounding seabed soil around the pipeline. The pipeline sinks downward relative to its initial

position at the early stage, regardless of transporting crude oil or natural gas, until to the moment when the upward buoyancy applied on the pipeline become greater than the gravity of the pipeline-oil/gas system. After that the pipeline continuously floats up driven by the significant buoyancy. It is noted that the magnitude of floating displacement of the pipeline transporting natural gas is much greater than the pipeline transporting crude oil due to the much lighter weight of natural gas than that of crude oil. This substantial floating of the pipeline-gas system extrudes the seabed soil over the pipeline with a more obvious way, making the seabed over the pipeline hunch more significantly than that if crude oil is transported.



(a) Dissipation of pore pressure and growth of effective stress



(b) Subsidence of pipeline

Fig. 23. The subsidence of the pipeline in the post-consolidation process.

- (3) Two effective stress-based criteria are proposed to judge the occurrence of soil liquefaction. Their own advantages and disadvantages all have been presented in the study. Adopting the two criteria, the liquefaction zone in the seabed soil closed to the pipeline is successfully predicted. It is found that the surrounding seabed soil around the pipeline does not become liquefied. Only the soil in the upper seabed with shallow depth away from the pipeline becomes liquefied with a liquefaction depth 1.2–1.5 m. Additionally, the shapes and the sizes of the liquefaction zone predicted adopting the two proposed effective stress-based criteria are basically the same without significant difference. It is indicated that the two effective stress-based criteria adopting  $L_p$  and  $|I_1|$  are both acceptable to predict the liquefaction zone surrounding the pipeline.
- (4) Through the comparative analysis between the pipeline-oil-seabed system and the pipeline-gas-seabed system, it is found that the biggest difference on the dynamics of the pipeline and its surrounding seabed soil between them is reflected on the upward floating of the pipeline driven by the excess pore pressure induced by hydrodynamic loading. Secondly, the magnitude of dilation of the seabed soil under the pipeline transporting natural gas is much greater than that if crude oil is transported.
- (5) There is basically little attention has been paid on the consolidation process of seabed foundation after wave stopping to apply in previous literature. The post densification process of the pipeline-oil/gas-seabed system is firstly presented in this study. It will promote us to further understand the mechanism and dynamics characteristics of offshore pipeline subjected to ocean wave hydrodynamic loading.
- (6) The computational results show that the integrated mode FSSI-CAS 2D has successfully and subtly captured a series of nonlinear physical phenomena of the intensive interaction between the pipeline transporting crude oil or natural gas and the loosely deposited seabed soil, e.g., the vibration, sinking and floating of the pipeline, the large deformation, liquefaction in the surrounding seabed soil etc. It is indicated that the integrated model FSSI-CAS 2D developed by Ye et al. (2013b) and Jeng et al. (2013) has an advantage to investigate the complicated interaction between fluid-structure-seabed foundation.
- (7) It is essential to point out that this work is just an early work in the field of numerical analysis of the dynamics of submarine pipelines, as well as in the area of evaluation of the stability of submarine pipelines under hydrodynamic load. The main purpose is to comprehensively understand the basic mechanism how a pipeline buried in loose seabed floor responds to hydrodynamic

load under some ideal conditions. There should be certain gap with the application in practical engineering, because either there are a number of conditions set in the numerical modelling are slightly different with the realistic conditions, or some important factors that could affect the dynamics of pipelines are not taken into consideration in this study, e.g. the complex topography of seabed floor affected by scouring, the effect of pipeline laying (ploughing or jetting, backfilling) on the mechanical properties of the surrounding soil of pipelines, and the axial effect on the behaviour of pipelines (upheaval bulking) caused by the operational defects in the process of pipeline laying.

### CRedit authorship contribution statement

**Jianhong Ye:** Conceptualization, Methodology, Investigation, Formal analysis, Writing – review & editing, Writing – original draft, Writing, Supervision, Funding acquisition. **Kunpeng He:** Visualization.

### Declaration of competing interest

The authors declare that they have no known competing financial interests or personal relationships that could have appeared to influence the work reported in this paper.

### Acknowledgements

Professor Jianhong YE is grateful to the funding support from National Natural Science Foundation of China under project NO. 51879257.

### References

- Bayraktar, D., Ahmada, J., Larsena, B.E., Carstensen, S., Fuhrman, D.R., 2016. Experimental and numerical study of wave-induced backfilling beneath submarine pipelines. *Coast Eng.* 118, 63–75.
- Berghe, J.F.V., Cathie, D.N., Ballard, J.C., 2005. Pipeline uplift mechanisms using finite element analysis. In: *Proceedings of the 16th International Conference on Soil Mechanics and Geotechnical Engineering*, pp. 1801–1804.
- Bizzotto, T., Brown, M., Brennan, A., Powell, T., Chandler, H.W., 2017a. Modelling of pipeline and cable flotation conditions. In: *Proceedings of the 8th Offshore Site Investigation and Geotechnics International Conference*, 2, pp. 865–871.
- Bizzotto, T., Brown, M.J., Powell, T., Brennan, A.J., Chandler, H., 2017b. Toward less conservative flotation criteria for lightweight cables and pipelines. In: *Proceedings of the 27th International Ocean and Polar Engineering Conference*, vol. 2. ISOPE, pp. 535–540.
- Bransby, M.F., Newson, T.A., Brunning, P., Davies, M.C.R., 2001. Numerical and centrifuge modelling of the upheaval resistance of buried pipelines. In: *Proceedings of the 20th International Conference on Offshore Mechanics and Arctic Engineering*. OMAE01/PIPE–4118.
- Cathie, D.N., Jeack, C., Ballard, J.C., Wintgens, J.F., 2005. Pipeline geotechnics – state-of-the-art. In: Cassidy, G. (Ed.), *International Symposium of Frontier in Offshore Geotechnics*, pp. 95–114.
- Chan, A.H.C., 1988. A Unified Finite Element Solution to Static and Dynamic Problems of Geomechanics. PhD thesis. University of Wales, Swansea Wales.
- Cheng, A., 1986. Seepage force on a pipeline buried in a poroelastic seabed under wave loading. *Appl. Ocean Res.* 8 (1), 22–32.
- Cheuk, C.Y., White, D.J., Bolton, M.D., 2008. Uplift mechanisms of pipes buried in sand. *J. Geotech. Geoenviron. Eng.* 134 (2), 154–163.
- Christian, T.J., Taylor, P.K., Yen, J.K.C., Erali, D.R., 1974. Large diameter underwater pipeline for nuclear plant designed against soil liquefaction. In: *Proceedings of Offshore Technology Conference*, pp. 597–606. Houston.
- Cowie, M., Finch, M., 2001. Backfill improvement techniques - optimising pipeline burial solutions. In: *Proceedings of Offshore Technology Conference*, pp. OTC–13142. Houston, Texas, USA.
- Duan, L., Liao, C.C., Jeng, D.S., Chen, L., 2017. 2D numerical study of wave and current-induced oscillatory non-cohesive soil liquefaction around a partially buried pipeline in a trench. *Ocean Eng.* 135, 39–51.
- Dunn, S.L., Vun, P.L., Chan, A.H.C., Damgaard, J.S., 2006. Numerical modeling of wave-induced liquefaction around pipelines. *J. Waterw. Port, Coast. Ocean Eng.* 132 (4), 276–288.
- Fredsoe, J., 2016. Pipeline–seabed interaction. *J. Waterway, Port, Coast, Ocean Eng.* ASCE 142 (6), 03116002.
- Herbich, J.B., Schiller, R.E., Dunlap, W.A., Watanabe, R.K., 1984. *Seafloor Scour, Design Guidelines for Ocean-Founded Structures*. Marcel Dekker, New York.
- Hsu, T.J., Sakakiyama, T., Liu, P.L.F., 2002. A numerical model for wave motions and turbulence flows in front of a composite breakwater. *Coast Eng.* 46, 25–50.
- Jeng, D.-S., Ye, J.H., Zhang, J.-S., Liu, P.-F., 2013. An integrated model for the wave-induced seabed response around marine structures: model, verifications and applications. *Coast Eng.* 72 (1), 1–19.
- Kammerer, A.M., Wu, J., Pestana, J.M., Riemer, M., Seed, R.B., 2000. *Cyclic Simple Shear Testing of Nevada Sand for Peer Center Project 2051999*. Technical Report, University of California. Patent, Berkeley, CA.
- Kiziloz, B., Cevik, E., Yuksel, Y., 2013. Scour below submarine pipelines under irregular wave attack. *Coast Eng.* 79, 1–8.
- Larsen, B.E., Fuhrman, D.R., Sumer, B.M., 2016. Simulation of wave-plus-current scour beneath submarine pipelines. *J. Waterw. Port, Coast. Ocean Eng.* 142 (5), 04016003.
- Liao, C.C., Zhao, H., Jeng, D.S., 2015. Poro-elasto-plastic model for the wave-induced liquefaction. *J. Offshore Mech. Arctic Eng.* 137 (4), 042001.
- Liu, B., Jeng, D.S., 2016. Laboratory study for influence of clay content (cc) on wave-induced liquefaction in marine sediments. *Mar. Georesour. Geotechnol.* <https://doi.org/10.1080/1064119X.2015.1005322> (in press).
- Luan, M., Qu, P., Jeng, D.S., Guo, Y., Yang, Q., 2008. Dynamic response of a porous seabed-pipeline interaction under wave loading: soil-pipeline contact effects and inertial effects. *Comput. Geotech.* 35, 173–186.
- MacPherson, H., 1978. Wave forces on pipeline buried in permeable seabed. *J. Waterw. Port, Coast. Ocean Div.* 104 (4), 407–419.
- Magda, W., 1992. Wave-induced pore pressure acting on a buried submarine pipeline. *Proceedings of 23rd International Conference on Coastal Engineering*, pp. 3135–3148.
- Martin, G.R., Seed, H.B., 1984. One-dimensional dynamic ground response analyses. *J. Geotech. Eng. ASCE* 108 (7), 935–952.
- Miyamoto, J., Sassa, S., Sekiguchi, H., 2004. Progressive solidification of a liquefied sand layer during continued wave loading. *Geotechnique* 54 (10), 617–629.
- Miyamoto, J., Sassa, S., Tsurugasaki, K., Sumida, H., 2020. Wave-induced liquefaction and floatation of a pipeline in a drum centrifuge. *J. Waterway, Port, Coast, Ocean Eng.* ASCE 146 (2), 04019039.
- Neelamani, S., Ai-Banaa, K., 2012. Variation in wave forces on buried submarine pipeline in different types of soils in random waves. In: *Proceedings of the ASME 2012 31st International Conference on Ocean, Offshore and Arctic Engineering*, pp. OMAE2012–83018.
- Newson, T.A., Deljouei, P., 2006. Finite element modelling of upheaval buckling of buried offshore pipelines in clayey soils. In: *Proceedings of the GeoShanghai International Conference-Soil and Rock Behavior and Modeling*, pp. 351–358.
- Pastor, M., Chan, A.H.C., Mira, P., Manzanal, D., Fernandez, M.J.A., Blanc, T., 2011. Computational geomechanics: the heritage of olek zienkiewicz. *Int. J. Numer. Methods Eng.* 87 (1–5), 457–489.
- Pastor, M., Zienkiewicz, O.C., Chan, A.H.C., 1990. Generalized plasticity and the modelling of soil behaviour. *Int. J. Numer. Anal. Methods Geomech.* 14, 151–190.
- Powell, T., Fisher, R., Phillips, R., Jee, T., 2002. Reducing backfilling risks. In: *Offshore Site Investigation and Geotechnics: Diversity and Sustainability*. London, pages SUT–OSIG–02–175.
- Roy, K., Hawlader, B., Moore, 2018. Uplift failure mechanisms of pipes buried in dense sand. *Int. J. GeoMech.* 18 (8), 04018087.
- Sassa, S., Sekiguchi, H., 1999. Wave-induced liquefaction of beds of sand in a centrifuge. *Geotechnique* 49 (5), 621–638.
- Sassa, S., Takayama, T., Mizutani, M., Tsujio, D., 2006. Field observations of the build-up and dissipation of residual porewater pressures in seabed sands under the passage of stormwaves. *J. Coast Res.* 39, 410–414.
- Seed, H.B., Rahman, M.S., 1978. Wave-induced pore pressure in relation to ocean floor stability of cohesionless soils. *Mar. Geotechnol.* 3 (2), 123–150.
- Sumer, B.M., Fredsoe, J., Christensen, S., Lind, M.T., 1999. Sinking/floatation of pipelines and other objects in liquefied soil under waves. *Coast Eng.* 38 (2), 53–90.
- Summer, B.M., Hatipoglu, F., Fredsoe, J., Hansen, N.E.O., 2006a. Critical flotation density of pipelines in soils liquefied by waves and density of liquefied soils. *J. Waterway, Port, Coast, Ocean Eng.* ASCE 132 (4), 252–265.
- Summer, B.M., Truelsen, C., Fredsoe, J., 2006b. Liquefaction around pipeline under waves. *J. Waterw. Port, Coast. Ocean Eng.* 132 (4), 266–275.
- Teh, T.C., Palmer, A.C., Bolton, M.D., Damgaard, J.S., 2006. Stability of submarine pipeline on liquefied seabeds. *J. Waterway, Port, Coast, Ocean Eng.* ASCE 132 (4), 244–251.
- Teh, T.C., Palmer, A.C., Damgaard, J.S., 2003. Experimental study of marine pipelines on unstable and liquefied seabed. *Coast Eng.* 50 (1–2), 1–17.
- Turcotte, B., 1984. *Laboratory Evaluation of Wave Tank Parameters for Wave-Sediment Interaction*. Cornell University, August.
- Wu, J., Kammerer, A.M., Riemer, M.F., Seed, R.B., Pestana, J.M., 2004. Laboratory study of liquefaction triggering criteria. In: *Proceedings of 13th World Conference on Earthquake Engineering*. British Columbia, Vancouver, Canada. Paper No. 2580.
- Yang, G.X., Ye, J.H., 2017. Wave & current-induced progressive liquefaction in loosely deposited seabed. *Ocean Eng.* 142, 303–314.
- Yang, G.X., Ye, J.H., 2018. Nonlinear standing wave-induced liquefaction in loosely deposited seabed. *Bull. Eng. Geol. Environ.* 77 (1), 205–223.
- Ye, J.H., 2012. *Numerical Analysis of Wave-Seabed-Breakwater Interactions*. PhD thesis. University of Dundee, Dundee, UK.
- Ye, J.H., Jeng, D.S., 2012. Response of porous seabed to nature loadings: waves and currents. *J. Eng. Mech.* ASCE 138 (6), 601–613.
- Ye, J.H., Jeng, D.-S., Liu, P.L.-F., Chan, A.H.C., Wang, R., Zhu, C.-Q., 2014. Breaking wave-induced response of composite breakwater and liquefaction of seabed foundation. *Coast Eng.* 85, 72–86.

- Ye, J.H., Jeng, D.-S., Wang, R., Zhu, C.-Q., 2013a. Numerical study of the stability of breakwater built on sloped porous seabed under tsunami loading. *Appl. Math. Model.* 37, 9575–9590.
- Ye, J.H., Jeng, D.-S., Wang, R., Zhu, C.-Q., 2013b. Validation of a 2D semi-coupled numerical model for Fluid-Structures-Seabed Interaction. *J. Fluid Struct.* 42, 333–357.
- Ye, J.H., Jeng, D.-S., Wang, R., Zhu, C.-Q., 2015. Numerical simulation of wave-induced dynamic response of poro-elasto-plastic seabed foundation and composite breakwater. *Appl. Math. Model.* 39, 322–347.
- Ye, J.H., Wang, G., 2015. Seismic dynamics of offshore breakwater on liquefiable seabed foundation. *Soil Dynam. Earthq. Eng.* 76, 86–99.
- Ye, J.H., Wang, G., 2016. Numerical simulation of the seismic liquefaction mechanism in an offshore loosely deposited seabed. *Bull. Eng. Geol. Environ.* 75 (3), 1183–1197.
- Zhang, X.L., Jeng, D.S., Luan, M.T., 2011. Dynamic response of a porous seabed around pipeline under three-dimensional wave loading. *Soil Dynam. Earthq. Eng.* 31, 785–791.
- Zhang, Y., Ye, J.H., He, K.P., Chen, S.G., 2019. Seismic dynamics of pipeline buried in dense seabed foundation. *J. Mar. Sci. Eng.* 7 (6), 190.
- Zhao, K., Xiong, H., Chen, G.X., Zhao, D., Chena, W., Du, X., 2018. Wave-induced dynamics of marine pipelines in liquefiable seabed. *Coast Eng.* 140, 100–113.
- Zhou, C.Y., Li, G.X., Dong, P., Shi, J.H., Xu, J.S., 2011. An experimental study of seabed responses around a marine pipeline under wave and current conditions. *Ocean Eng.* 38, 226–234.
- Zhou, X.L., Jeng, D.S., Yan, Y.G., Wang, J.H., 2013. Wave-induced multi-layered seabed response around a buried pipeline. *Ocean Eng.* 72, 195–208.
- Zienkiewicz, O.C., Chan, A.H.C., Pastor, M., Schrefler, B.A., Shiomi, T., 1999. *Computational Geomechanics with Special Reference to Earthquake Engineering*. John Wiley and Sons, England.
- Zienkiewicz, O.C., Chang, C.T., Bettess, P., 1980. Drained, undrained, consolidating and dynamic behaviour assumptions in soils. *Geotechnique* 30 (4), 385–395.